

(4)

CHEMICAL
RESEARCH,
DEVELOPMENT &
ENGINEERING
CENTER

DTIC FILE COPY

CRDEC-TR-88088

AD-A199 732

ION CONTENT OF MOIST ATMOSPHERIC
AIR AND THE MOLECULAR STRUCTURE OF
WATER VAPOR THUS INFERRED

S DTIC
ELECTED
SEP 29 1988
D

by Hugh R. Carlon
U.S. Army Fellow

RESEARCH DIRECTORATE

July 1988



U.S. ARMY
ARMAMENT
MUNITIONS
CHEMICAL COMMAND

DISTRIBUTION STATEMENT A
Approved for public release
Distribution Unlimited

Aberdeen Proving Ground, Maryland 21010-5423

88 9 29 046

Disclaimer

The findings in this report are not to be construed as an official Department of the Army position unless so designated by other authorizing documents.

Distribution Statement

Approved for public release; distribution is unlimited.

UNCLASSIFIED

SECURITY CLASSIFICATION OF THIS PAGE

REPORT DOCUMENTATION PAGE				Form Approved OMB No. 0704-0188
1a. REPORT SECURITY CLASSIFICATION UNCLASSIFIED		1b. RESTRICTIVE MARKINGS		
2a. SECURITY CLASSIFICATION AUTHORITY		3. DISTRIBUTION/AVAILABILITY OF REPORT Approved for public release; distribution is unlimited.		
2b. DECLASSIFICATION/DOWNGRADING SCHEDULE				
4. PERFORMING ORGANIZATION REPORT NUMBER(S) CRDEC-TR-88088		5. MONITORING ORGANIZATION REPORT NUMBER(S)		
6a. NAME OF PERFORMING ORGANIZATION CRDEC		6b. OFFICE SYMBOL (If applicable) SMCCR-RSP	7a. NAME OF MONITORING ORGANIZATION	
6c. ADDRESS (City, State, and ZIP Code) Aberdeen Proving Ground, MD 21010-5423		7b. ADDRESS (City, State, and ZIP Code)		
8a. NAME OF FUNDING/SPONSORING ORGANIZATION CRDEC		8b. OFFICE SYMBOL (If applicable) SMCCR-RSP	9. PROCUREMENT INSTRUMENT IDENTIFICATION NUMBER	
8c. ADDRESS (City, State, and ZIP Code) Aberdeen Proving Ground, MD 21010-5423		10. SOURCE OF FUNDING NUMBERS		
		PROGRAM ELEMENT NO	PROJECT NO	TASK NO
				WORK UNIT ACCESSION NO
11. TITLE (Include Security Classification) Ion Content of Moist Atmospheric Air and The Molecular Structure of Water Vapor Thus Inferred				
12. PERSONAL AUTHOR(S) Carlton, Hugh R., U.S. Army Fellow				
13a. TYPE OF REPORT Technical	13b. TIME COVERED FROM 86 May TO 87 May	14. DATE OF REPORT (Year, Month, Day) 1988 July	15. PAGE COUNT 46	
16. SUPPLEMENTARY NOTATION				
17. COSATI CODES		18. SUBJECT TERMS (Continue on reverse if necessary and identify by block number)		
FIELD 04	GROUP 02	SUB-GROUP	Moist Air, Water Clusters : Nucleation Water Vapor, Hydrogen bonding, Evaporation Ions : Electrical Conductivity, Infrared (IR)	
20	05			
19. ABSTRACT (Continue on reverse if necessary and identify by block number)				
<p>A great deal of multidisciplinary research, reported in the open literature, suggests that even the cleanest water vapor is not simply a collection of single water molecules (monomers) as is popularly supposed, but also contains vast populations of molecular aggregates of clusters especially under conditions of high humidity. These "water clusters" include not only collision-induced, Boltzmann-distributed dimers, trimers, etc., but also a preponderance of much larger evaporatively-produced clusters that are extensively hydrogen bonded and thus form equilibrium populations in the vapor. The question of the extent of such clustering in the vapor versus temperature and humidity has been investigated in rigorous new measurements of the electrical conductivity of moist air. The ion populations measured in the vapor give excellent agreement with those predicted by equations developed from first principles of kinetic theory. These ion populations are dissociative products of the large clusters. The ions stabilize the clusters at (continued on reverse)</p>				
20. DISTRIBUTION/AVAILABILITY OF ABSTRACT <input checked="" type="checkbox"/> UNCLASSIFIED/UNLIMITED <input type="checkbox"/> SAME AS RPT <input type="checkbox"/> DTIC USERS		21. ABSTRACT SECURITY CLASSIFICATION UNCLASSIFIED		
22a. NAME OF RESPONSIBLE INDIVIDUAL SANDRA J. JOHNSON		22b. TELEPHONE (Include Area Code) (301) 671-2914	22c. OFFICE SYMBOL SMCCR-SPS-T	

UNCLASSIFIED

18. Subject Terms (continued)

Atmosphere
Clouds
Fogs
Cloud Physics

19. Abstract (continued)

equilibrium by aggregating additional monomers. The data are highly reproduceable and indicate that as saturation is approached, particularly in the presence of vigorous water droplet generation, virtually all water monomers in the vapor can be involved in clustering at any instant of time. That is, complete clustering of water vapor in the presence of evaporating liquid water can be approached particularly under energetic conditions of evaporation. This behavior exists even in stagnant, closed systems containing liquid water and its vapor like those used to measure fundamental physical properties of water such as saturation vapor pressure. The discussion leads to conclusions, based on a solid body of new experimental evidence supporting basic theory from classical first principles, that require fundamental changes in our perceptions of water-substance.

PREFACE

The work described in this report was authorized under U.S. Secretary of the Army Science and Engineering Fellowship. This work was started in May 86 and completed in May 87.

The use of trade names or manufacturers' names in this report does not constitute an official endorsement of any commercial products. This report may not be cited for purposes of advertisement.

Reproduction of this document in whole or in part is prohibited except with permission of the Commander, U.S. Army Chemical Research, Development and Engineering Center, ATTN: SMCCR-SPS-T, Aberdeen Proving Ground, Maryland 21010-5423. However, the Defense Technical Information Center and the National Technical Information Service are authorized to reproduce the document for U.S. Government purposes.

This report has been approved for release to the public.

Accession No.	
NTIS No.	
DTIC File No.	
Storage Location	
Jackfile	
B.	
Distribution	
Availability	
Cost	Avg. Cost
A-1	



Blank

CONTENTS

	Page
1. INTRODUCTION	7
2. EXPERIMENTAL CONSIDERATIONS AND THE APPARATUS	9
3. EXPERIMENTAL PROCEDURE AND RESULTS (PART I).	14
4. THEORY AND DISCUSSION.	20
5. EXPERIMENTAL RESULTS (PART II)	35
6. CONCLUSIONS.	42
LITERATURE CITED	45

LIST OF FIGURES

Figure No.		Page
1	Experimental Apparatus. (View A) Overall Front Oblique View (View B) Rear Oblique View Showing Close-up of Cell in Box, Insulators in Saddle, and Gasketed Cell-Acess Port.	12
2	Schematic Diagram of Electrical Measurement Circuit for Cell, Showing Bias Source, Voltmeter and Cell Connected in Series . . .	13
3	Data Plots of Voltmeter Reading, E_v , vs. Saturation Ratio ($s = \% \text{ RH}/100$), for Humidification	16
4	Ion Population, I_{cc} , Measured at 28 °C in Moving Air vs. Saturation Ratio	17
5	Data Plot of Voltmeter, E_v , vs. Saturation Ratio	18
6	Data Plot of Voltmeter, E_v , vs. Saturated Ratio.	19
7	Mass Spectra Measured ³⁴ for Constant Temperature 100 °C and 1 atm Total Pressure	22
8	Compilation of Mass Spectral Data ³⁴ Over a Range of Temperature and Saturation Ratio ($s = \% \text{ RH}/100$) Conditions that are Indicated Values Next to the Points.	24
9	M_{av} , The Average "Effective Molecular Weight" of Water Vapor vs. Saturation Ratio ($s = \% \text{ RH}/100$)	31
10	"P," In mm Hg (Torr), The vapor pressure that water vapor would have if it actually consisted of all monomers	33
11	Data Plots of Voltmeter Reading, E_v , vs. Supply Voltage, E_b , for Increasing Bias Voltages $E_b = 0.1 - 2.0 \text{ kV}$ Under Conditions of an Initially Wet Box	37
12	Data Plots of Voltmeter Readings, E_v , vs. Saturation Ratio Obtained by First Heating Moist Air in an Initially Wet Box to a Maximum Temperature of 33 °C.	38

ION CONTENT OF MOIST ATMOSPHERIC AIR AND THE MOLECULAR STRUCTURE OF WATER VAPOR THUS INFERRED

1. INTRODUCTION

Liquid water is extensively structured due to hydrogen bonding. The bonds form molecular aggregates or "clusters" that comprise the liquid.¹ Luck² deduced that at 25 °C, for example, 85% of liquid water is clustered at any instant of time. Water exhibits a much smaller (10⁻⁶ to 10⁻⁵ times) rate of evaporation than would be expected from kinetic theory; yet, this theory works very well for unassociated substances such as mercury.³ The heat of vaporization and surface tension of water are much larger than those of other substances. This behavior is consistent with the extensive clustering due to hydrogen bonding in the liquid and is generally explained on these grounds.

Water vapor is usually assumed to consist of a vast majority of single molecules (monomers) and perhaps traces of Boltzmann-distributed dimers, trimers, etc. Our present homogeneous nucleation theory⁴ is based on this view. In his classical cloud chamber studies^{5,6} that were carried out before hydrogen bonding was known to exist, C.T.R. Wilson wondered at the vast numbers ($> 10^8/\text{cm}^3$ of vapor) of large uncharged clusters he produced in his experiments that served as nuclei for the condensation of his "cloud-like" water droplets. Because these clusters had radii three times larger than the accepted radius for the water monomer and because monomer collision and momentary "sticking" was the only clustering mechanism that accommodated classical kinetic theory, Wilson suggested that perhaps the known molecular (monomer) radius was in error by a factor of three. He wrote:⁵ "... it is difficult to account for the immense number of these nuclei, otherwise than on the view that they actually are simply small aggregates of water molecules, such as may come into existence momentarily through encounters of the molecules. On this view the dimensions of the molecules cannot be small compared with 6×10^{-8} centim....." The radius of the water molecule is, of course, 2×10^{-8} cm.

In retrospect, Wilson understood these phenomena better than the cloud microphysicists that succeeded him and produced elaborate theories to explain observed behavior in water vapor.⁷ These theories were hypothesized but never proven, because the droplets grown large enough for optical detection and studied in the cleanest vapor contained 10⁷ more monomers than the molecular aggregates or "water clusters" from which they had been nucleated. Seven orders of magnitude could scarcely be accommodated without introducing serious questions in the interpretation of experimental data, however carefully taken.

The physical interface between liquid water and its vapor, through which pass the species that determine fundamental physical properties of water such as saturation vapor pressure and surface tension, is poorly understood. DeBoer³ stated if this surface behavior was as expected from classical theory, many lakes and seas would evaporate in a few hours and the oceans would be dry in a few days. Croxton⁸ devotes a short chapter to the subject, after stating

in a prologue that any statistical mechanical theoretical treatment of the water surface presents particularly formidable problems and, indeed, that such a discussion of these interfacial properties might well be "premature."

But through all of this, no one has seriously proposed that water vapor, particularly when saturated, might be extensively structured by populations of liquid-like molecular water clusters having size distributions corresponding to equilibria established for particular temperature and partial pressure conditions. Theory, if unchallenged, eventually becomes accepted; once accepted, it becomes unchallengeable. Perhaps that has happened in our evolution of such theories stemming from C.T.R. Wilson's original, brilliant experimental work.^{5,6} While Wilson went on to further accomplishments, the heirs to his discoveries were gradually leading us further astray.

There is evidence in the literature that cluster activity exists in water vapor and moist air. In infrared (IR) water vapor absorption measurements, Bignell⁹ extended the work of Varanasi, et al.¹⁰ to show anomalous or excessive absorption that had a quadratic partial pressure and an inverse temperature dependence and was attributed to molecular structure in the vapor. Quite naturally, the water dimer was suggested as the possible cause. This led to a long and continuing series of investigations of this infrared "continuum absorption" that is observed in wavelength intervals where the water monomer has no absorption. Gebbie¹¹ and his co-workers, who organized a concerted attack on this problem, reported that anomalous absorption in the atmosphere at ambient temperatures was not attributable to equilibrium water dimers. In 1978, the IR water vapor continuum absorption was proposed to have a "molecular interpretation" based on hydrogen bonding in the vapor,¹² but no specific mechanisms were postulated. Completely unexpected behavior of steam-generated, cooling water fog clouds was reported¹³ in 1979 in IR radiometric spectral emission studies, which was explained as due to large clusters existing in large numbers in warm water vapor. Researchers also reported in 1979 that the observed temperature dependency of the infrared continuum absorption could be calculated almost precisely from the square root of the dissociative ion product of liquid water and that simple molecular oscillator models could be used to calculate the IR continuum absorption by assuming that distributions of large water clusters could exist in the atmosphere.¹⁴ The ability to model the continuum absorption from the dissociative ion product led to the present work.

Millimeter-wave absorption by fogs shows intense activity by unknown species.¹⁵ Commenting on these observations and their variability, Gebbie¹⁶ proposed a metastable cluster of about size 50 monomers to explain the absorption and yet to conform to accepted kinetic and nucleation theories. He did not, however, investigate the possible existence on large, stable equilibrium populations of hydrogen-bonded clusters in the vapor that easily could have explained these data.

At what size, or number of monomers comprising it, does a water cluster in the vapor begin to exhibit the thermodynamic properties of liquid water? Studies of water clusters using crossed-beam techniques¹⁷ show that when a cluster comprises about six or more monomers, its near-infrared absorption spectrum closely resembles that of liquid water. Castleman and his co-workers,¹⁸ in extensive measurements of entropy and other thermodynamic properties of water ion clusters of the structure $H^+(H_2O)_n$, found that clusters of

size $n = 4$ to 6 or more are, thermodynamically, liquid water. Thus, water clusters nearly 10 times smaller than the critical size needed for droplet nucleation already behave like liquid "plets" in the vapor and can impart to the vapor liquid-like behavior including IR continuum and millimeter-wave spectral absorption, and electrical properties that are the subject of the present work. It is also known that when liquid water and saturated moist air at atmospheric pressure, however clean, exist together at temperatures above about 50°C , water droplets will begin to appear in the vapor.¹⁹ These droplets are nucleated "spontaneously", even in the absence of foreign nuclei in the vapor, and their numbers steadily increase as the atmospheric boiling point is approached. This means that even in the most careful measurement of such fundamental physical properties of water as its saturation vapor pressure at temperatures above 50°C , droplets and evaporatively-produced clusters like $(\text{H}_2\text{O})_n$ must always be present, and that their populations increase with increasing temperature. Thus, the saturated vapor is to some extent clustered and this clustering will, according to kinetic theory, proportionately reduce the measured equilibrium vapor pressure. Investigated in the present work are (1) the extent clustering also occurs in the saturated vapor at temperatures below 50°C in the absence of droplets large enough for optical detection and (2) a description of this clustering as a function of temperature and saturation in water vapor; i.e., what fraction of all monomers in the vapor is involved in clustering at any instant of time?

2. EXPERIMENTAL CONSIDERATIONS AND THE APPARATUS

Electrification of water vapor or moist air by evaporating liquid, particularly if the evaporation is energetic, attracted the interests of theoreticians and experimentalists for over two centuries. Volta²⁰ may have been the first to suggest, in 1782, that electrical charges are liberated by evaporating water. Faraday²¹ knew by 1844 that jets of escaping wet steam can produce strong electrification. In 1892, Lenard²² discovered that the splashing of water produces charging, while in the early 1900's other workers^{23,24} observed charging from the violent breaking of droplets that depended to some extent upon dissolved substances, but they could not measure electrification due to the gradual production of a new water surface. Blanchard²⁵ showed that ions can be generated by bursting water bubbles.

The author,²⁶ in 1980, first reported the very large ion populations that can be generated in closed containers by boiling water. Data were taken using electrical conductivity cells of a new kind, which used compensation for insulator leakage currents. The electrical conductivity cells basic design is still being used in the present work with further refinements. Measurements were extended to conditions of simple evaporation of stagnant water,²⁷ and it was learned that boiling was not necessary to produce very large ion populations in moist air, although boiling did produce larger populations than did simple evaporation. This strengthened the view that the ions were simply being continuously generated as dissociative products from a vastly larger population of evaporating neutral water clusters that had much longer lifetimes than did the ion charges. As often happens when sophisticated measurements become routine, sources of error can be reintroduced into experiments. For large conductivity cells of the type described below and in references 26-28, the conductivity of the water ions in moist air or water vapor between the cell plates and that

due to leakage through thin films of water that condense on insulator surfaces becomes comparable.

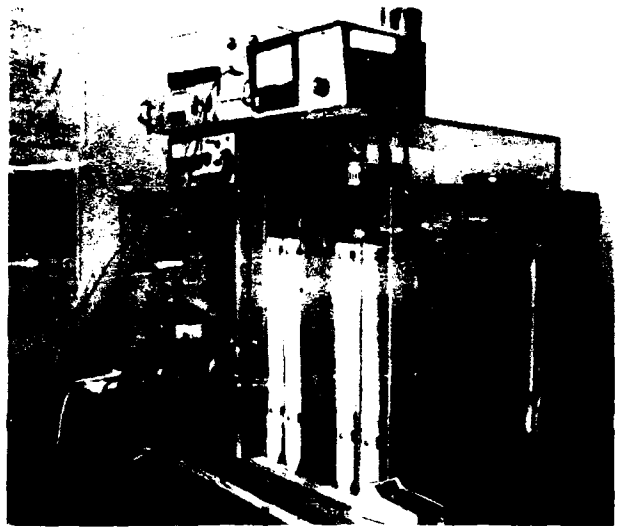
Both show a very steep dependence upon humidity that is nearly identical for the insulators and for the vapor itself. Moore²⁹ only discusses the insulator effects. Investigations with better insulators and improved mechanical cell designs²⁸ confirmed that a new design that effectively eliminated the insulators as a source of experimental error was required if unequivocal data were to be obtained giving true ion populations in the vapor, particularly in conditions approaching saturation at higher temperatures. This design, proven in the present work, will now be discussed.

The apparatus is shown in Figure 1. A lucite box 105 cm long by 35 cm wide by 46 cm high contains the vapor conductivity test cell or capacitor, probes to measure dry bulb temperature and dew point, a 10 cm diameter muffin fan that provides air circulation at about 1 m/s when desired, a 600 cc pyrex beaker containing a 500 W immersion heater, and three plastic tubes that can be used to deliver cool fog from an external ultrasonic nebulizer into the box, liquid water into the beaker, or liquid water on the floor of the box, respectively. A Yellow Springs Instrument Co., Model 91 HF calibrated precision electronic dew point hygrometer is connected to the probes and provides a direct meter readout of dew point and air temperature in the box. It gives precision readings with the fan on or off, after stabilizing to one or the other condition for 3-5 min. The muffin fan is Dayton Model 100. The external ultrasonic nebulizer, a medical instrument, is a Bennett Model US-1 that provides energy control settings on a scale from 0 to 10 to determine the fog output rate. The vapor conductivity test cell or simply the "cell" will be discussed in detail below. Lucite was chosen for the apparatus wall material as it has been used for many years in earlier work²⁶⁻²⁸ with no detectable difficulties. Lucite allows visual examination of water vapor condensation on the walls that are often wet during experiments except under the heated saddle as discussed below. A 10 cm hole in the end of the box opposite the cell allows access for tubes and wires and is sealed during experiments that are carried out at atmospheric pressure. The box otherwise is sealed with rubber gaskets and wing nuts on threaded studs around two access panels that are used, e.g., to remove or service the cell or to clean the box.

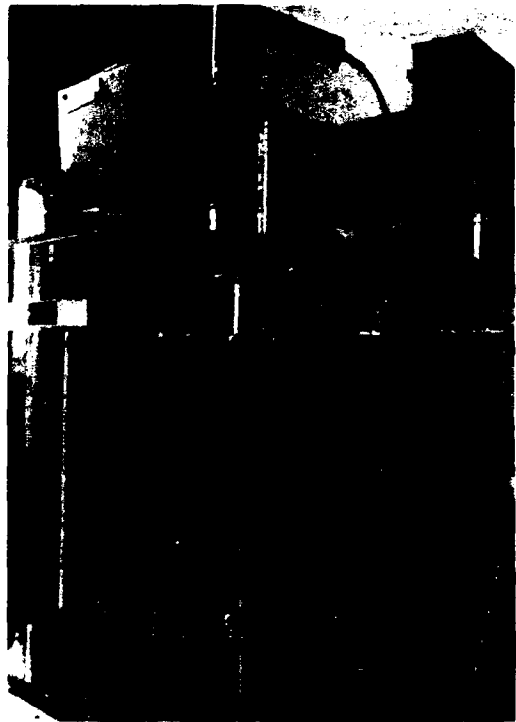
The cell consists of 40 square aluminum plates (26.5 cm on a side) with an average separation of 0.66 cm between the plates. Alternative plates are electrically connected to pairs of threaded steel rods that carry the weight of the plates and to which leads can be connected for conductivity readings. The steel rods pass through small (1.3 cm diameter) clearance holes in the walls of the box to the insulators, which are vertical strips of polytetrafluoroethylene (PTFE) (1.3 cm thick by 2.5 cm wide by 39 cm long) and are machined to sharp points at their bottom ends. The points rest on PTFE shims that are used to center the steel rods in the clearance holes. There are two sets of 20 plates each, carried on their own steel rods and insulators that are intertwined but otherwise are not in direct physical contact. Thus, the two sets of plates can be adjusted horizontally by moving the insulators and vertically by using the shims, to avoid contact between the rods and clearance holes, and between the two sets of nested plates.

The insulators are enclosed in a removable duct or "saddle" that is used to control their environment and to keep them dry during experiments. This is the novel feature of the new design compared to earlier designs,²⁶⁻²⁸ and it yields unequivocal experimental results. Since the same water species that are in the vapor also condense on and contaminate the insulators and since liquid water surface films on the insulators will have a much greater density than the vapor, insulator leakage can confuse experimental results unless eliminated because it has the same functional dependencies on temperature and water vapor partial pressure as does the electrical conductivity of the vapor. This fact has led to the current widespread misunderstanding that insulator effects, not vapor conductivity, are thought to explain atmospheric static electric space charge dissipation for various humidities.²⁹ By eliminating the insulator effects altogether, as in the present work, understanding of the true state of things is revealed.

The saddle is 32 cm wide and 5 cm thick along the side walls of the box where the insulators are housed and the steel rod clearance holes are located. At its top, the saddle has a plenum with a height of 10 cm above the top of the box, and a hole is provided at its top center to mount a two-heat (600/1200 W) domestic hair dryer. The 600 W dryer setting has proved adequate for all experiments to date. Contained in the plenum are a Cole-Parmer Instrument Co. (CP) Model 3310-40 certified temperature and relative humidity (RH) indicator, and a precision CP Model 3310-20 RH indicator. In operation, typical conditions monitored in the plenum with the dryer operating at 600 W are 70 °C and 13-15% RH. The dryer produces a slight overpressure in the saddle. This results in a net airflow through the cell rod clearance holes and into the box, thus, further insuring that moist air in the box during experiments does not even reach the insulators in the saddle, much less their pointed bottoms, to confuse the vapor conductivity data. The bottom of the saddle on both sides of the box is left open to the atmosphere, allowing hot air from the dryer to flow down the insulators, across the insulator points and the PTFE shims upon which the points rest, and back into the atmosphere. An electronic thermometer, Electromedics Inc., Model M-99, monitors the air temperature at the insulator points and shims as it leaves the saddle. Readings of 50 °C are typical here. In most experiments, it is standard practice to maintain a differential of at least 6 °C between the temperature at the insulator points and shims in the saddle and the dew point in the box although differences of 20 °C or more are common. But even if the saddle dry air and box dew point temperatures are permitted to approach one another, insulator leakage effects are rarely seen due to the extremely conservative design of the apparatus shown in Figure 1.



VIEW A



VIEW B

Figure 1. Experimental apparatus. (View A) Overall Front Oblique View (View B) Rear Oblique View Showing Close-up of Cell in Box, Insulators in Saddle, and Gasketed Cell-Access Port.

The water ion populations in water vapor, moist air, or on insulator surfaces are strongly dependent on RH as will be shown conclusively in the discussion of experimental results that follows. Thus, if the RH in the saddle is held only 20% below that in the box during a given experiment, the insulator leakage can be reduced by a factor of 20 times below what its value would be if the insulators were inside the box instead of outside in the saddle. At ambient conditions, even a saddle temperature as little as 6 °C above the dew point, temperature measured in the box would give an RH in the saddle 30% below that in the box. This would result in a 100 times insulator leakage reduction in the saddle compared to that if the insulators were in the box. Most experimental conditions are even more conservative than these, therefore, it can be stated with certainty that the electrical properties of the vapor in the box can be measured unequivocally even under extremes of temperature and humidity. These were precisely the experimental capabilities needed to evaluate the equations and theory discussed below.

Because of the large dimensions of the cell and thus its sensitivity to ions in the vapor, the simple electrical circuit shown in Figure 2 can be used. The cell is wired in series with a 0-400 V direct current (dc) highly-regulated power supply (Schlumberger Model SP-2719) and a Schlumberger Model SM-5228 vacuum-tube voltmeter (VTVM) that has a constant dc input impedance (resistance) of 11 megohms regardless of the voltage scale used. Thus, the supply voltage is simply divided between the VTVM and cell resistances, and the ion population is easily determined as discussed below. Even at 400 V dc, the supply voltage is smaller than that required to dissociate water molecules (monomers) or clusters into ions. This was verified by measuring voltages for a given moist air sample over a wide range of dc supply voltages. The response was linear over the entire range 0-400 V dc. To make certain that the applied supply or "bias" voltage did not deplete the ion populations measured between the cell plates, it was standard practice to apply the bias only momentarily for a voltage reading to be made. Continuous bias, if used, would reduce the ion populations by about 25-30%.

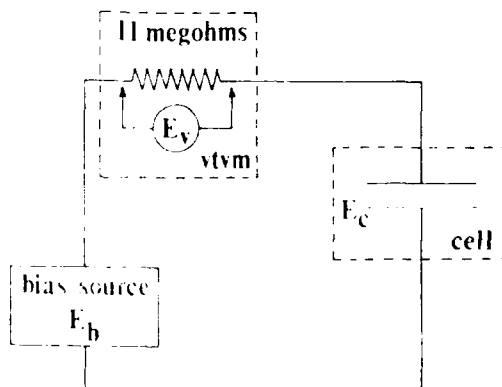


Figure 2. Schematic Diagram of Electrical Measurement Circuit for Cell, Showing Bias Source, Voltmeter and Cell Connected in Series.

Under the very diversified experimental conditions described below, voltages ranging from 0.01 to 20 or more V dc were recorded. These correspond to vapor ion populations ranging from a few hundred per cubic centimeter, as are commonly found in atmospheric air at about 50% RH, to about $10^6/\text{cm}^3$ under saturation conditions (100% RH) at temperatures above ambient. The muffin fan, which operates in some experiments, contributes several hundred ions per cubic centimeters to the vapor. But, these are short-lived ions whose effects are seen as rapid fluctuations of a few hundredths of a volt about the true dc voltmeter reading. If desired, the fan can be switched off momentarily for a reading, in which case a stable dc voltage corresponding to the ion population in the box is read. As RH is increased, these ion fluctuations due to the muffin fan motor quickly become negligible in the much larger voltages that results.

Several kinds of experiments can be conducted using the apparatus described here. These will be discussed as their data and results are presented in the two sections (parts) of this paper that follow.

3. EXPERIMENTAL PROCEDURE AND RESULTS (PART I)

While all experimental data reported here are extremely reproducible, the most precise data have been taken using the ultrasonic nebulizer to humidify the box shown in Figure 1. In a typical experiment, starting with a dry box, the humidity is gradually increased by nebulizing a cool water mist or fog through a plastic tube and into the box. The increases in humidity and voltage readings are carefully monitored at intervals of one minute or less. As the humidification proceeds and the humidity increases, the recorded voltage and its equivalent vapor ion content rise very steeply. The functional dependence of this increase at a given temperature is the thirteenth power of the saturation ratio ($s = \%RH/100$). That is, the voltmeter reading and the equivalent water ion content per cubic centimeter of vapor, both increase as $(s)^{13}$. If the muffin fan in the box is operating, the vapor mixture in the box is homogeneous and the data points cluster closely about the line $f(s)^{13}$ as shown in Figure 3A. If the fan is switched off, the data points tend to lie below the $f(s)^{13}$ line as humidification begins, but they "catch up" as humidity increases; this is shown in Figure 3B. The data in Figure 3 are entirely representative of those taken in one experiment after another. They have not been handpicked from a body of data; they are simply representative. A thirteenth-power functional dependence might at first seem exceptional in nature, but where molecular species are concerned it is commonplace. For example, the dependence of water's partial pressure upon temperature, $f(T)^n$, is $n = 13.2$ over the range $T = 273 - 546 \text{ K}$, and 17.9 over the range $293 - 303 \text{ K}$.

Figure 3 shows that operating the fan helps to shorten the time required to stabilize conditions in the box and perhaps slightly to enhance evaporation of the nebulized liquid water droplets. Furthermore, the rate of stabilization depends on the rate of evaporation as determined by the nebulizer energy setting. This is shown in Figure 4, where the ordinate shows the ion population measured per cubic centimeter of vapor. Equations giving this and other relationships are derived from first principles in the next section of this paper. Figure 4 shows the nebulizer energy control settings for a scale of 0-10 indicated by points on the dashed curves. At the lowest nebulizer setting used in the experiment considered here (setting = 2), the vapor ion population could not be maintained as humidification progressed. The next

higher nebulizer setting 3 allowed the solid $f(s)^{13}$ curve to be regained with increasing humidity; but again, the input rate was insufficient to maintain maximum values with further increases in s . At settings of 4 and 5 the nebulizer was able to maintain the vapor ion populations even at high humidities, and at settings of 6-7, still larger ion counts were recorded. Finally, at the maximum nebulizer energy setting 10, a maximum ion population near 10^6 ions/cm³ of vapor was recorded in saturation ($s = 1$). The solid curve in Figure 4 has the same slope as the curves in Figure 3 and, as will be shown in the next section, its intercept at $s = 1$ can be predicted from basic kinetic theory. Thus, it seems clear from highly reproducible experiments such as these that if sufficient energy is inputted to evaporate and maintain liquid droplets in the vapor, liquid in this case by using ultrasonic energy, a maximum ion population can be attained. It is also found that this ion population cannot be exceeded no matter how much additional energy is inputted at a given temperature. Small perturbations can be made to occur, but these disappear rapidly once the source of additional energy is removed.

Once humidification is complete, or nearly so in these experiments, it is instructive to raise the temperature of the vapor sample in the box and thus reduce the saturation ratio s (= %RH/100). This is conveniently done by operating the dryer atop the saddle for a prolonged period of time. It was mentioned previously that there is a small net flow of warm, dry air from the saddle and into the box through the clearance holes that accommodate the steel rods carrying the cell plates. By continuously operating the dryer at 600 W, the temperature of the moist air in the box is gradually raised as its saturation ratio is reduced. The solid curves in Figures 3 and 4 are slightly sensitive to temperature, rising with increasing temperature as the equations in the next section will show. Hence as the air is dried back down to lower humidities, the data points tend to rise slightly above a curve representing lower starting temperatures as is shown in Figure 3A. Any source of evaporating water is found to closely reproduce the same $f(s)^{13}$ dependence of voltage and ion population versus s as is obtained using the nebulizer. For example, Figure 5 shows data points for the rapid humidification of moist air in the box by operating the 500 W immersion heater in the 600 cm³ breaker so as to produce very energetic, violent boiling. The data points are more widely scattered than those Figures 3 and 4 (even though the fan was operating), especially above the solid $f(s)^{13}$ curve, but the trend of the data is almost exactly the same as when the nebulizer is used. The opposite, non-energetic, extreme is evaporation of standing water from the floor of the box, where it can be introduced through a plastic tube at a given starting time for an experiment. Typical results are shown in Figure 6, for data taken with the fan operating. Just as for the nebulizer at lower energy settings (Figure 4), evaporating standing liquid water is at first unable to produce equilibrium voltages and vapor ion populations as humidification proceeds. But above $s = 0.8$ (80% RH), humidification slows and becomes asymptotic to about $s = 0.9$ (90% RH). At the same time, the voltage and ion population increase to values on the solid curve, rising almost independently of humidity near $s = 0.9$. The humidity will not exceed about $s = 0.9$ unless energetic means are employed to evaporate more water, e.g., nebulization or boiling of the liquid. As expected, heating of the moist air causes the data points in Figure 6 to retrace the solid curve, rising slightly above this curve with increasing temperature. In fact, hysteresis-like effects are seen as moist air is dried by mixing with warmer, drier air with standing liquid water present. The vapor is, in effect,

"noisy", as is readily observed by voltmeter readings or, for that matter, in IR radiometry of warm water vapor or moist air.¹³ This noise does not originate from instrumental artifacts or experimental problems but is simply manifested by the vapor itself.

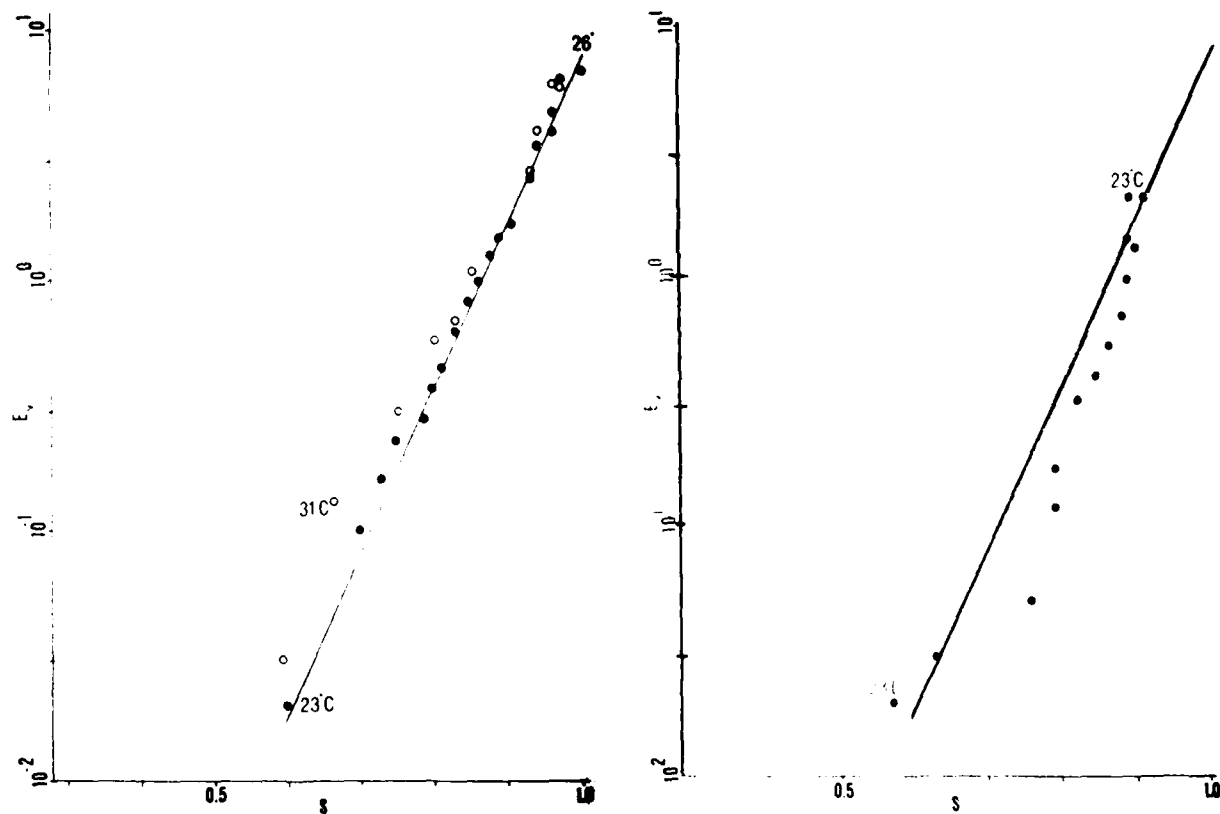


Figure 3. Data Plots of Voltmeter Reading, E_v , vs. Saturation Ratio ($s = \% \text{ RH}/100$), for Humidification

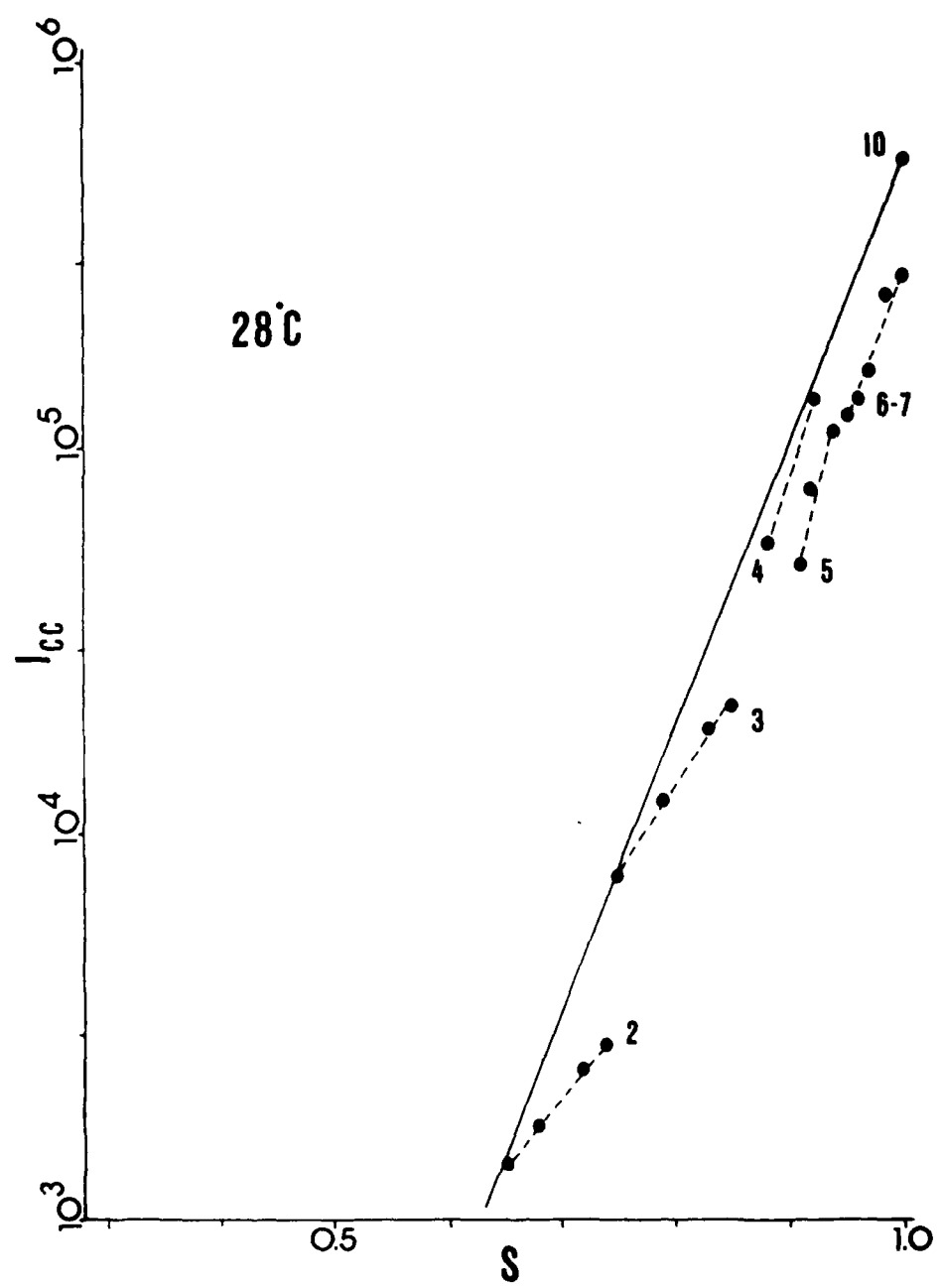


Figure 4. Ion Population, I_{cc} , Measured at 28 °C in Moving Air vs. Saturation Ratio

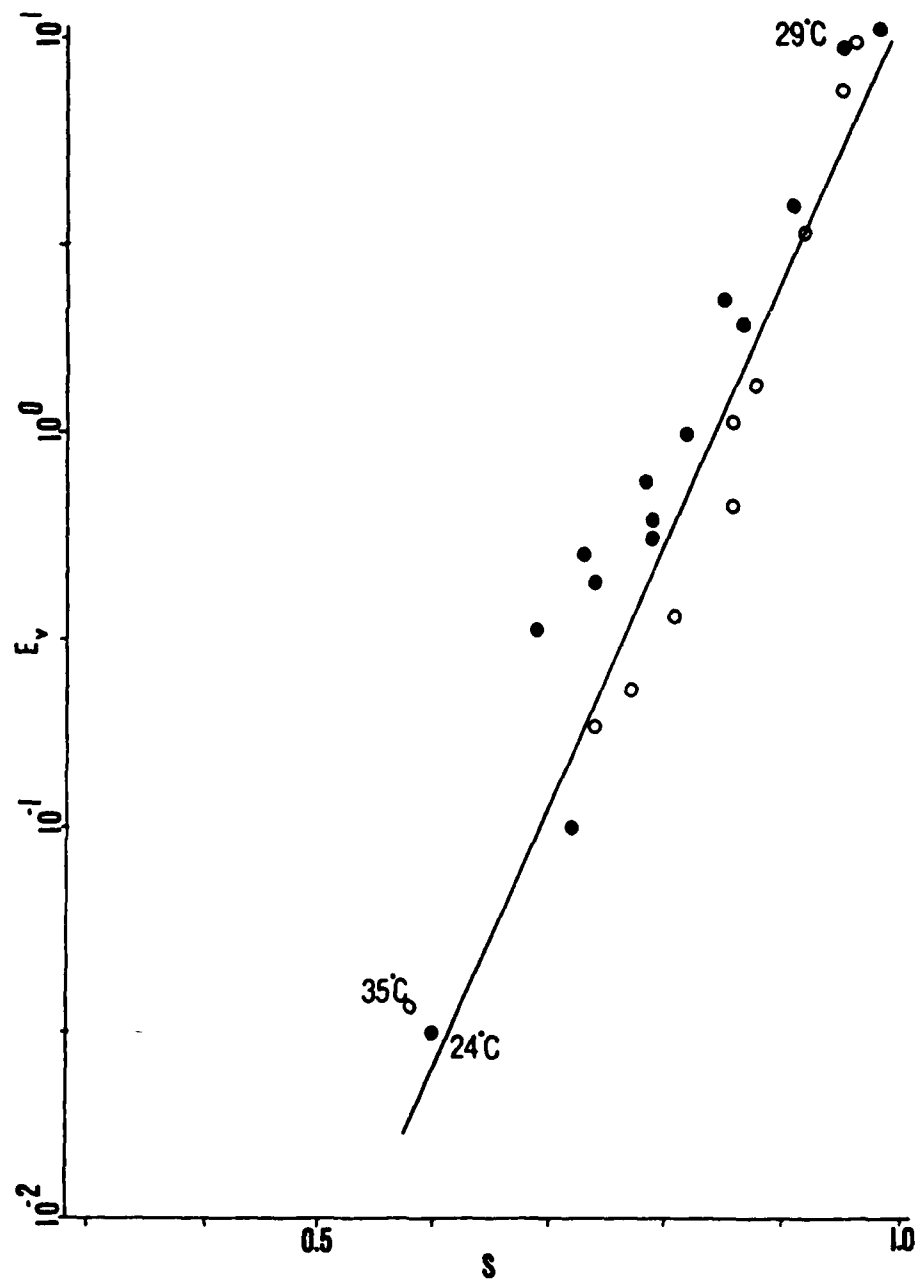


Figure 5. Data Plot of Voltmeter, E_v , vs. Saturation Ratio

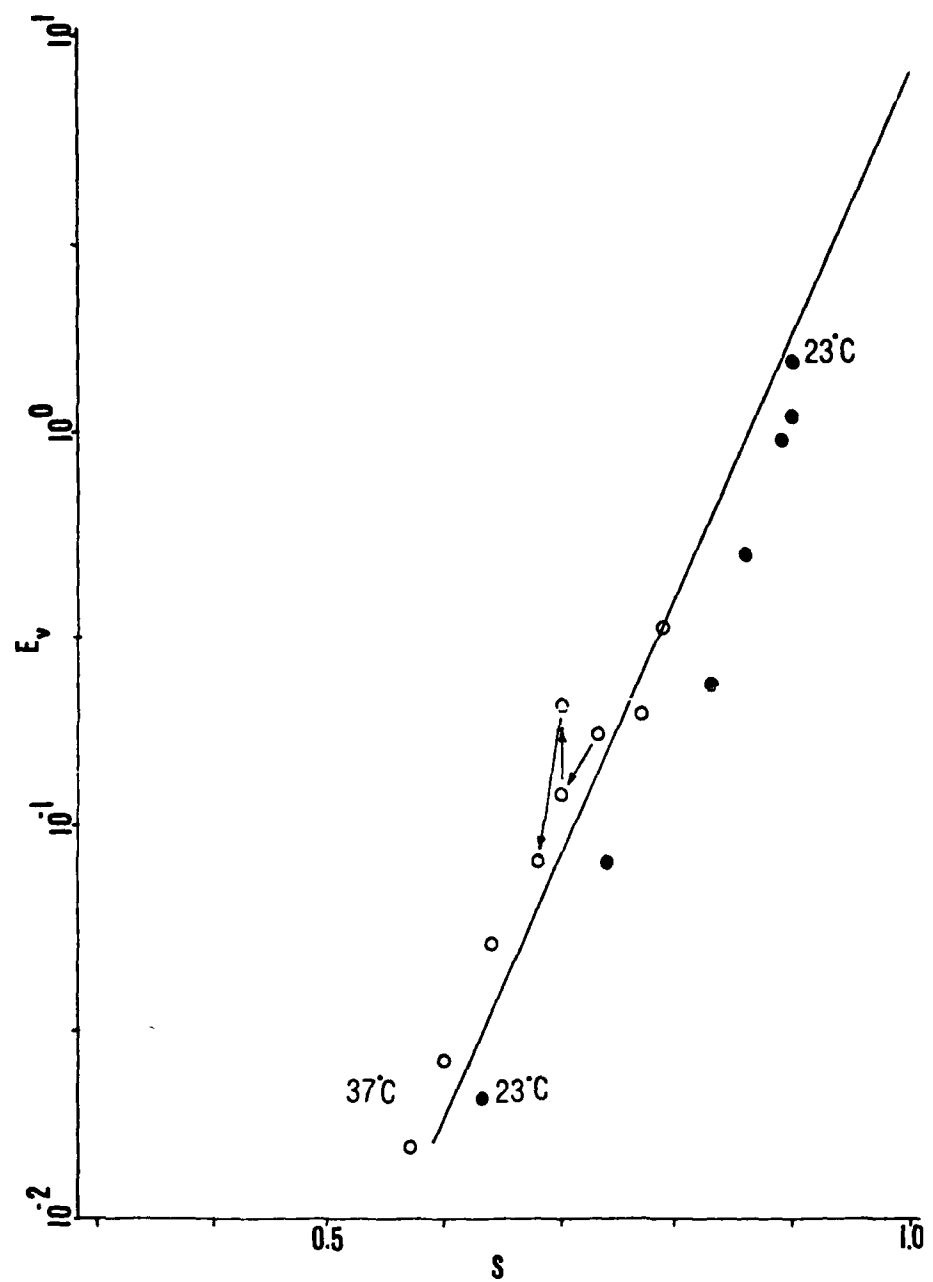


Figure 6. Data Plot of Voltmeter, E_v , vs. Saturated Ratio

In other experiments now being carried out at UMIST, moist air in the box was slowly humidified using the nebulizer at low energy settings. The air in the box was stagnant (the fan was switched off). Cell voltages were very carefully measured until some desired humidity was reached. The nebulizer was then switched off, and the humidity was allowed to fall slowly back to ambient conditions as the cell voltages were monitored in still air. The data points were found to rise and fall with humidification and drying along or around the expected $f(s)^{13}$ curve, but these points did not, themselves, form a smooth curve. Rather, little steps or "zig zags" were observed that are believed to correspond to changes in the size distributions and populations of the cluster species in the vapor that account for all of the phenomena discussed in this paper, including the ion populations measured in these experiments. These recent data and experimental results, as well as all of the results discussed above, are entirely consistent with the view that $f(s)^{13}$ is an equilibrium function for water vapor ion content versus humidity and that, while perturbations do occur about equilibrium, particularly under conditions of vigorous boiling or slow evaporation of liquid water, equilibrium is recovered within a few minutes. The nature of the dynamic equilibrium discovered will be discussed in the remaining sections of this paper. Two important points are noted here.

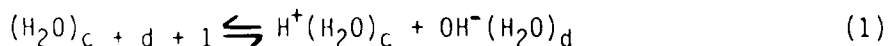
- (1) Equilibrium water ion populations in the troposphere will always obey an $f(s)^{13}$ dependence on the saturation ratio ($s = \%RH/100$), as shown in Figures 3-6. Thus, all reported observations of unusually high water ion content in the atmosphere must correspond to higher-humidity conditions, e.g., those of Faraday²¹ in wet steam and Blanchard²⁵ in the presence of bursting water bubbles. For example, in Figure 4 for moist air at 28 °C, the equilibrium population of 10^4 water ions/cm³ could only be measured at relative humidities of 77% ($s = 0.77$) or more. Thus, these curves give fundamental equilibrium relationships for water ion populations always to be expected in water vapor or moist tropospheric air.

- (2) The $f(s)^{13}$ dependency of water ion population on humidity, and the fact that the populations it predicts cannot be exceeded at atmospheric pressure except under non-equilibrium conditions, shows quite clearly that there are implications here concerning the fundamental physics of water-substance itself. If the measured ions are dissociative products of much larger populations of uncharged or neutral molecular aggregates ("water clusters") in water vapor, then it would appear that the populations of these water clusters also reach some maximum or "saturation" (equilibrium) population condition corresponding to that of the ions. But what could cause this saturation of the neutral water cluster populations? We are now in a position to suggest the answers to this and other questions.

4. THEORY AND DISCUSSION

Continuum-like IR and millimeter-wave spectral absorption that can be attributed to hydrogen-bonded neutral (uncharged) molecular clusters in water vapor has been known to exist for many years.^{9,11,12,15,16,30} The populations of these clusters per cubic centimeter of water vapor or moist air that are required to explain the magnitude of this absorption are many orders of magnitude larger than the populations of ion clusters per cubic centimeter measured in the present work. For example, at 25 °C in vapor at 70% RH, we measure about 3×10^3 water ions/cm³ of vapor at equilibrium. But, the

number of neutral clusters needed to explain the IR continuum absorption under these conditions is $5 \times 10^{14}/\text{cm}^3$, even if these are large aggregates of 10 or 15 monomers. If they were simply collision induced dimers, trimers, etc., still larger populations would be required to explain the absorption. In fact, neutral clusters of mean size 12 monomers in the vapor would outnumber the ion clusters at any instant of time by a factor of 10^{11} , i.e., eleven orders of magnitude. Thus, it is impossible to explain the absorption on any other grounds than that enormous populations of neutral water clusters exist in the vapor. Since the IR continuum absorption is directly proportional to the measured ion content of the vapor,³¹ it thus follows that the ions measured in the vapor are dissociative products of the comparatively huge neutral cluster populations. A remarkably simple mechanism also enters into this process. As the ions are formed, they are immediately "swarmed" by monomers or other clusters or ions in the vapor.³² This swarming tends to rebuild a cluster that has just dissociated to produce ions. Thus, a dynamic equilibrium is established between larger neutral clusters that are evaporating by dissociation, some of which produce ions in the process, and the water ions thus produced which immediately grow-larger. Since the neutral water cluster population per cubic centimeter is $> 10^{11}$ larger than the water ion population per cubic centimeter of vapor, this infers that the lifetimes of large, hydrogen-bonded neutral clusters are much longer than the ion charge lifetimes, which are of the microsecond time-scale or longer.³³ The populations of water ion clusters in the vapor are dependent upon the thirteenth power of the saturation ratio, s ($= \%RH/100$). Thus, the dynamics of clustering and ionization in water vapor or moist air are truly impressive. The dynamic equilibrium in the vapor can be represented by the reaction:



where the most likely ionization event corresponds to $d = 0$, i.e., the loss of a single OH^- group perhaps as a "loose end" from a cluster. In this case, the cluster sizes for water ions $H^+(H_2O)_c$ would correspond approximately to neutral cluster sizes only one monomer larger, and the distributions of ion and neutral clusters would be very similar. The frequency of dissociative events like those in equation 1 can be greatly increased by subjecting a water vapor or moist air sample to e.g., β -irradiation as is commonly done in mass spectrometric investigations of water clusters to measure their thermodynamic properties.¹⁸ Examples of such mass spectra³⁴ are shown in Figure 7, where the caption gives further details of the experimental procedures. Conditions here were those in the presence of saturated vapor at somewhat lower temperatures, raised to 100°C at atmospheric pressure, resulting in the sub-saturated partial pressures shown. The clusters were allowed to form first and were only irradiated while being drawn through the pinhole of the mass spectrometer. Note that as the partial pressure (p , mm Hg) increases at constant temperature, the cluster size (c) of the distributions increases from a mean value (c_μ) of 11-12 at $p = 42$ mm, to about 15 at $p = 113$ mm, to about 25 at $p = 234$ mm. These conditions correspond at 100°C to, respectively, vapor saturation ratios ($s = \%RH/100$) of 0.056, 0.15 and 0.31. The "spike" at $c = 21$ in the upper mass spectrum indicates that the population of clusters of this size is favored in an otherwise Gaussian-like distribution because size 21 corresponds to a compact, low energy dodecahedron "clathrate" configuration comprising 20 monomers arrayed in a hydrogen-bonded pentagonal configuration (i.e., a configuration of pentagons) about a caged central monomer.

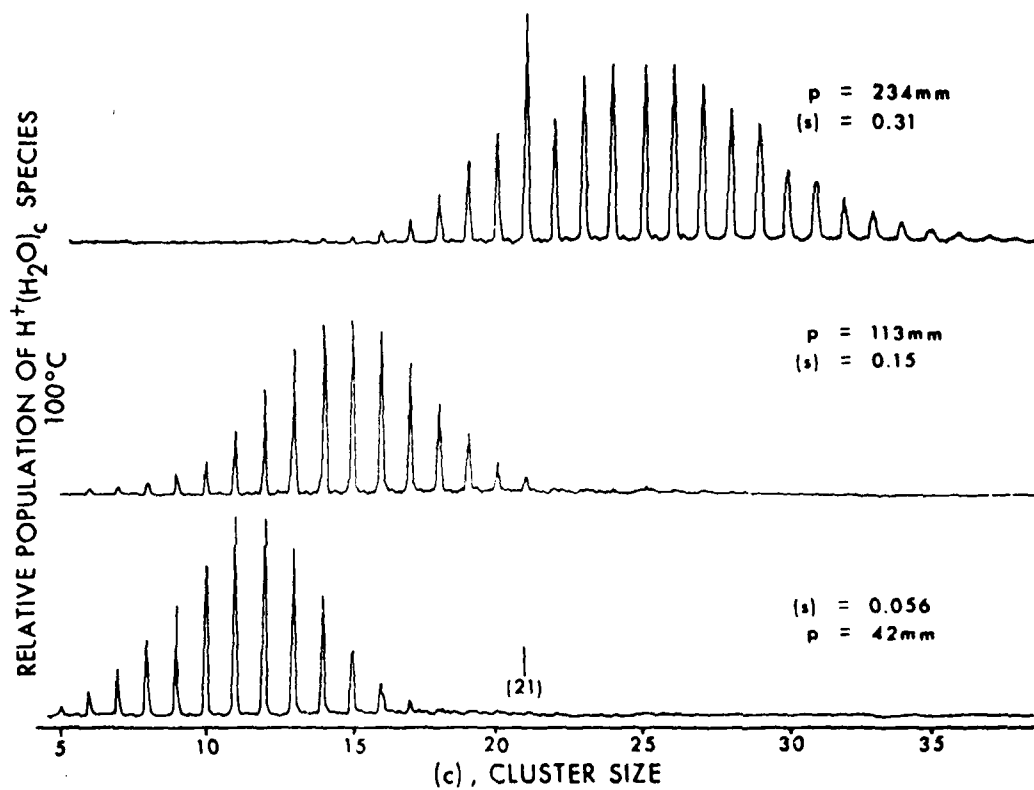


Figure 7. Mass Spectra Measured³⁴ for Constant Temperature 100 °C and 1 atm Total Pressure

Studies like these, both in saturated and sub-saturated moist air at many temperatures, have permitted the logical progression of mean cluster size, c_μ , versus temperature and partial pressure at atmospheric pressure to be deduced. The results are shown in Figure 8. Under saturated conditions ($s = 1$), it is found that the mean cluster size of the distribution is given by:

$$c_\mu = 0.44 T_k - 119.12 \quad (s = 1, 1 \text{ atm}) \quad (2)$$

where T_k is the Kelvin temperature and the constant 119.12 does not indicate five significant figures, but rather gives rounded values of c_μ for many temperatures. At 100 °C (373 K), this equation gives $c_\mu = 45$ as the mean size of the cluster distribution. This is the approximate size of a cluster configuration that could serve as the nucleus for droplet generation under all conditions.¹⁹ Thus, in saturation at the boiling point, there would be an unrestricted exchange of growing and evaporating liquid droplets through the critical size for nucleation.

It is also observed that the mean size of the cluster distribution under sub-saturated conditions can be approximated by:

$$\frac{c_\mu}{s} \approx c_\mu \sqrt{s} - 1 \text{ (atm)} \quad (3)$$

In Figure 8, experimental points are shown for $c_\mu = 12$ at $s = 1$, and for $\tilde{c}_\mu = 4$ at $s = 0.1$. Equation 2 and Figure 8 also indicate that at 0 °C, the atmospheric freezing point, the mean cluster size falls to unity denoting the monomer. This seems a consistent finding, because it is difficult to conceive of water clusters evaporating from the surface of bulk ice rather than from bulk liquid water. However, cluster sizes on the right-hand side of the near-Gaussian distribution could still exist at 0 °C. Their distribution would then appear to be Boltzmann-like, and these clusters could be confused with collision-induced ones.

We have no presently-accepted theoretical guidance to calculate the concentrations or populations of dissociative ions in water vapor. We have only experimental data and the well-known "dissociative ion product" of liquid water that will now be discussed. Liquid-like clusters of size 4-6 or larger have, as experiment has shown, the spectral¹⁷ and thermodynamic¹⁸ properties of bulk liquid water. Thus, extrapolation of the dissociative ion product of liquid water into the less-dense vapor phase, in the presence of large concentrations of liquid water and liquid-like clusters in the vapor phase, is defensible. Especially under energetic conditions of evaporation, this extrapolation would serve as a first approximation of the true state of affairs as concerns ionization of clusters in the vapor. It was mentioned that liquid water is approximately 85% hydrogen-bonded at any instant at 25 °C². There are no prima facie reasons why clusters in liquid water, momentarily segregated from neighboring clusters, might not themselves evaporate in addition to monomers from the liquid surface of standing water at ambient temperature, or even more likely

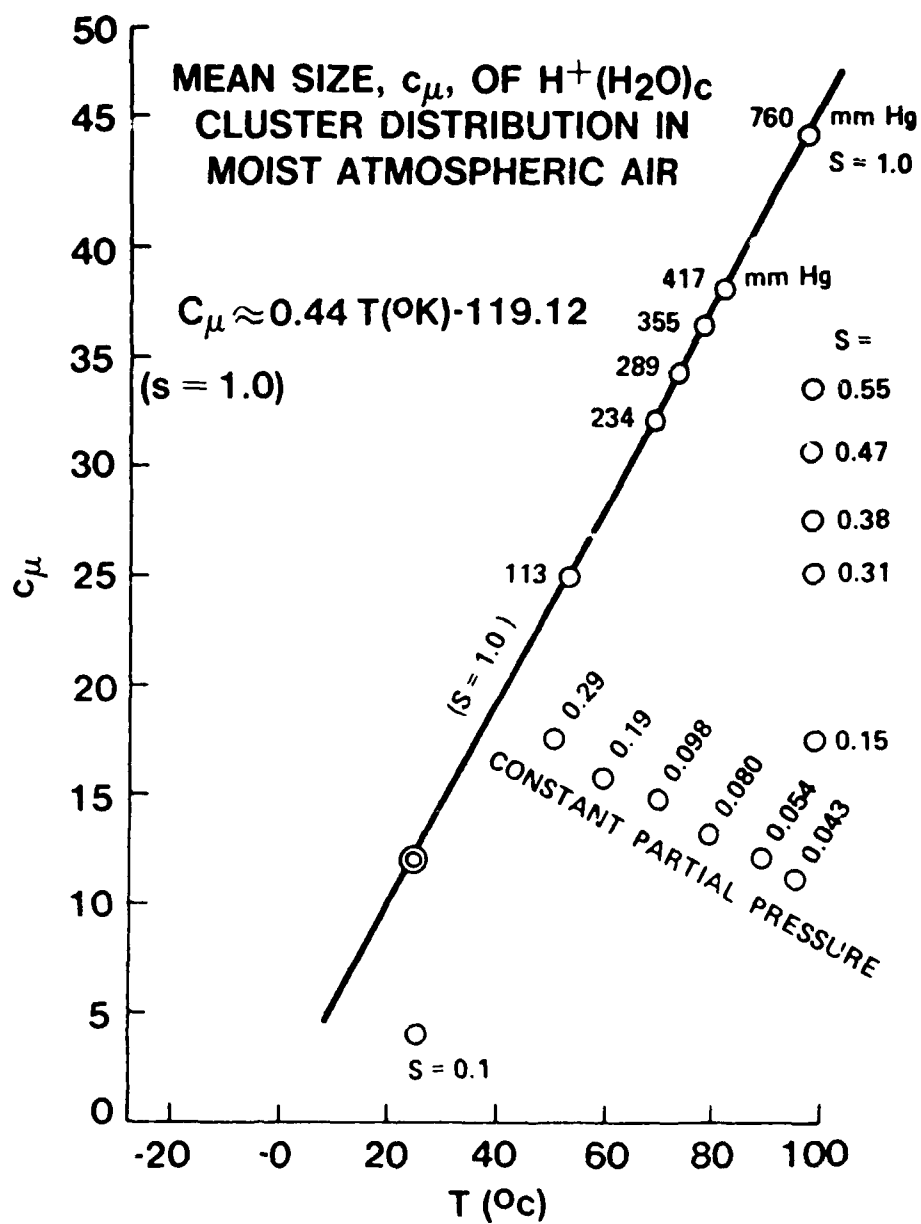


Figure 8. Compilation of Mass Spectral Data³⁴ Over a Range of Temperature and Saturation Ratio ($s = \% \text{ RH}/100$) Conditions that are Indicated Values Next to the Points

from liquid droplet surfaces in energetic systems. If simple evaporation of clusters occurs even from standing water, this would help to explain the great departures in the physical properties and behavior of water compared to most other substances that follow classical rules of kinetic theory. Examples have been cited by many including deBoer³ who indicated that if water behaved "normally", the seas would dry up in a few days, and Croxton⁸ who observed that a statistical-mechanical treatment of the liquid surface of water might be "premature". Such behavior, and that of the vapor over liquid water, might also explain the great discrepancies exhibited by water between its liquid and vapor phases in its abnormally low vapor pressure and its very large heat of vaporization.

The equilibrium constant for the slight dissociation of water if it proceeds according to equation 1 is given by:

$$K = a_{H^+}(H_2O)_c \cdot a_{OH^-}(H_2O)_d / a(H_2O)_{c+d+1} \quad (4)$$

where a is the molar concentration of a given species. Alternatively, these concentrations can be expressed in any other convenient units, including as the populations of total ions (I_{CC}) and neutral species (N_{CC}) per cubic centimeter of liquid water or on an individual cluster basis. Thus, if the ions and the neutral species are similar in size, one can also write:

$$K = \frac{I_{CC}^{\pm}}{N_{CC} \text{ liquid}} \quad (5)$$

For liquid water, the numerator of equation 4 is the dissociative equilibrium ion product, K_w ,³⁵ which can be expressed as a function of temperature by a rewritten form of the empirical expression deduced by Holzapfel:³⁶

$$K_w = \exp(-7156/T - 8.17) \quad (6)$$

where T is the absolute temperature (K). The denominator of equation 4 gives the concentration or population of the neutral water species that dissociate to form ions in equation 1, but it is taken as unity for the ion product because the degree of dissociation is so slight as to have negligible effect on the concentration or population of the neutral species per unit of volume of liquid water. Thus, the concentration or population per unit volume of one or the other ion is:

$$\sqrt{K_w} = a_{H^+}(H_2O)_c = a_{OH^-}(H_2O)_d \quad (7)$$

or if the ions are paired the total concentration or population of both species is:

$$2\sqrt{K_w} = a_{H^+}(H_2O)_c + a_{OH^-}(H_2O)_d = 2 \exp(-3578/T - 4.085) \quad (8)$$

The ratio of ions (right-hand side of equation 1) to neutral species (left-hand side of equation 1) in liquid water can be written in another form:

$$K' = 2 \sqrt{K_w} / a = 2 a^{\pm} / a = (I_{cc}/N_{cc})_{\text{liquid}} \quad (9)$$

where a^{\pm} and a are the concentrations of ions and neutral species, respectively, and I_{cc} and N_{cc} are the populations of these ions and neutral species per cubic centimeter of liquid, respectively. The extent of ionization is so slight at equilibrium that a and N_{cc} are considered unchanged. On an individual cluster basis (equation 1), $\sqrt{K_w}$ (or about 10^{-7} at room temperature) is considered simply as the probability that a given neutral cluster will ionize at any instant of time.

The step can now be taken to extrapolate the dissociative reaction of equation 1 from liquid water to the vapor in the absence of any other theoretical guidance. The ion population in the vapor will be much less per cubic centimeter than in the liquid, and so it is essential that a density correction be made. Since K' is the ratio of ions to neutral species in liquid water, we can define a similar ratio for the vapor phase. In the vapor, the ion and neutral species will have the form of aggregates or clusters of water molecules (monomers) moving randomly. The ion clusters will be far less populous than the neutral clusters, but the neutral clusters will still be liquid-like in the vapor. Their dissociation will still be much the same as in bulk liquid water where at any instant of time neutral clusters are to some extent independent of their neighboring clusters. In the vapor, however, these liquid-like "sites" are spaced much further apart than in the liquid. The extent of their ionization is still very slight compared to their overall population; hence the assumption that their loss of concentration or population in ionization is negligible remains valid. But, the vapor ion population will depend on the population or density of these species in the vapor compared to the liquid. Thus,

$$\frac{I_{cc}/N_{cc}}{a=1} \sim \frac{2 \sqrt{K_w}}{\rho_v} \cdot \frac{\rho_v}{\rho_L} \quad (10)$$

where ρ_v and ρ_L are the densities of the vapor and liquid phases, respectively. Since $\rho_v = PM/RT$,

$$\frac{I_{cc}/N_{cc}}{a=1} \sim 2 \sqrt{K_w} \cdot \frac{P M}{R T \rho_L} \quad (11)$$

where P is the vapor pressure in Torr (mm Hg), M is the molecular weight, R is the gas constant $62,360 \text{ cm}^3\text{-mm Hg/K g-mole}$, and T is the Kelvin temperature. The population of neutral clusters per cubic centimeter of vapor is:

$$N_{cc} = \frac{P N_A n_v}{R T c \mu(n_L)} \quad (12)$$

where N_A is Avogadro's number, c_μ is the mean size or mean number of monomers comprising a neutral cluster of average size in the vapor, and n_v and (n_L) are, respectively, the fractions of all water molecules that actually form neutral clusters at any instant of time in the vapor and in the liquid. (n_L) is shown in parentheses here as a reminder that, even though its values are known versus temperature,² its effects probably have already been included in standard measurements of the ion product, K_w , because the liquid cluster fraction at any temperature is a basic property of water and probably does affect the dissociative ion concentrations and populations. It is carried through the equations here so that it can be evaluated, if desired, in conservative calculations and as a reminder that it is the liquid-phase counterpart of the extremely important parameter n_v , the vaporphase equilibrium cluster fraction.

Experimental determination of n_v is the objective of the present work. All physical properties of water vapor at its interface with the liquid will depend on the vapor cluster fraction, n_v , and its magnitude particularly at saturation where many standard physical properties of water are measured. n_v would be expected to be considerably smaller than the fraction of liquid water clustered, (n_L) , at least in sub-saturated vapor, and it must be determined experimentally. IR and millimeter-wave measurements^{13,37} have shown that in water clouds or fogs approaching saturation conditions, values of n_v ranging from 0.03-0.07, and even occasionally as large as 0.2, have been inferred in order to adequately explain observed spectral absorption levels. There is much in the literature to suggest that at humidities approaching saturation, n_v has a very steep dependence upon humidity and makes prediction of the absorption almost impossible.^{13,15,16,31,37}

In equation 12, n_v corrects for the number of clustered water molecules per cubic centimeter of vapor, while c_μ divides these into N_{CC} clusters of that mean size diffused through the vapor containing $(1 - n_v)$ fraction of single water molecules or monomers. The effect of (n_L) , if it is considered at all, is slight particularly at normal ambient temperatures where it is not far from unity. Combining equations 11 and 12 gives:

$$I_{CC} \sim 2 \sqrt{K_w} \cdot \left(\frac{P}{RT} \right)^2 \frac{M N_A n_v}{\rho_L (n_L) c_\mu} \quad (13)$$

n_v can be determined experimentally from equation 13 because all other terms can be evaluated. c_μ is given by equations 2 and 3, (n_L) is near unity and has been discussed previously, and $2 \sqrt{K_w}$ is given by equation 8. I_{CC} is measured by electrical conductivity of the vapor, as will now be discussed.

The current density (j), A/cm^2 , for singly-charged ions is:

$$j = I_{CC} e u E, \quad (14)$$

where I_{CC} has already been defined as the number of ions per cubic centimeter of vapor at any instant, e is the value of the electronic charge ($1.6 \times 10^{-19} C$), u is the ion mobility (taken here as an average of $1 \text{ cm}^2/V \text{ sec}$ for an ion cluster of mean size c_μ), and E is the electric field strength (V/cm). For measurements of the electrical conductivity of water vapor or moist air, the direct current (dc) resistance or reciprocal conductance in megohms (R_{meg}) is related to I_{CC} by the equation:

$$I_{CC} = \frac{L}{A} \frac{x 10^{-6}}{R_{meg} e u} \quad (15)$$

where L is the plate spacing (cm) and A is the total plate area (cm^2) of an air-dielectric capacitor such as the one used by the author for experimental measurements to evaluate equation 12. Combining equations 13 and 15 and solving for n_v gives:

$$n_v \sim \frac{\rho L (n_L) c_\mu \times 10^{-6}}{2 \sqrt{K_w} R_{meg} e u M N_A} \left(\frac{L}{A} \right) \left(\frac{RT}{P} \right)^2 \quad (16)$$

Many of the terms in equation 16 can now be evaluated to give a theoretically-developed, numerical equation:

$$n_v \sim \frac{\rho L (n_L) c_\mu}{R_{meg}} \left(\frac{L}{A} \right) \left(\frac{T}{P} \right)^2 \exp \frac{(3578 - 2.708)}{T} \quad (17)$$

For the capacitor used in experiments to evaluate the theory and equations here, the 40 square metal plates comprising it were 26.5 cm on an edge, and there were 39 spaces between them with an average separation of 0.66 cm. Thus, $L = 0.66 \text{ cm}$ and $A = (26.5)^2 \times 39 = 27,388 \text{ cm}^2$. Using a simple series circuit consisting of a dc bias voltage source (Figure 2), the 40-plate capacitor and a vacuum-tube voltmeter having a constant 11 megohm dc input impedance, the electrical resistance of the vapor between the plates can be measured so that:

$$\frac{1}{R_{meg}} = \frac{1}{11 \left(\frac{E_b}{E_v} - 1 \right)} \quad (18)$$

where E_b and E_v are the dc bias voltage and the dc voltage measured by the voltmeter, respectively. Equation 17 can be reduced to final form for this experimental set-up:

$$n_v \sim \frac{\rho L (n_L) c_\mu}{E_b - 1} \left(\frac{T}{P} \right)^2 \times \exp \frac{(3578 - 15.74)}{T} \quad (19)$$

The right-hand side of equation 19 can be completely evaluated. For example, the usual bias voltage in these experiments was $E_b = 400 \text{ V dc}$. In saturated water vapor or moist air at atmospheric pressure at 25°C , ρ_L is near unity, $(n_L) = 0.85$, $c_\mu = 12$ (equation 2), $T = 298\text{K}$ and $P = 23.78 \text{ Torr}$. Equation 19 gives:

$$n_v \sim \frac{38.3}{25^\circ\text{C} \frac{400 - 1}{s = 1} E_v} \quad (20)$$

Thus for a voltmeter reading of, say, $E_v = 1$ V dc, the calculated fraction of cluster in the saturated vapor at 25 °C is 0.096, a result supportable, e.g., by IR radiometric spectral measurements of steam-generated fogs,¹³ or by millimeter-wave absorption spectra of natural fogs.^{15,37} Recent measurements at UMIST have routinely given voltmeter readings of 1 V dc or more. In fact, readings of 10 V dc or more can be obtained when water vapor is introduced into the test cabinet by boiling, or by using the ultrasonic nebulizer, at temperatures from 23-43 °C and saturation ratios approaching unity, i.e., approaching 100% relative humidity ($s = \%RH/100 + 1.0$). At smaller saturations, the extremely reproducible (s)¹³ dependency discussed previously is noted in the voltmeter reading, E_v , at a given temperature (Figures 3-6). When these data are investigated using equations 16, 17 and 19 for a wide range of values of (s) and temperature, it is found that they imply that n_v has a somewhat smaller, approximately 10th-power dependency on (s) and, furthermore (unlike E_v or I_{CC}), that n_v is almost independent of temperature at least over the range 23-43 °C, i.e.

$$n_v \sim (s)^{10} \quad (\text{at least over temperature range } 23-43 \text{ } ^\circ\text{C}) \quad (21)$$

This, a large and growing body of detailed experimental data indicates that: (1) in water systems near or at saturation, very large fractions of the vapor, n_v , can be involved in clustering especially with evaporating and condensing droplets present, and (2) the humidity dependence of n_v is very steep ($\sim(s)^{10}$) so that in typical atmospheres with 40-60% RHs ($s = 0.4-0.6$), the cluster fraction will be highly variable and its manifestations often will be masked by an overwhelming majority of single water molecules (monomers) and other contaminants in the case of the open atmosphere.

These observations suggested investigations of a converse kind. Suppose that energy is applied to a closed system containing liquid water and its vapor to whatever input level is desired, so long as destruction of species present does not occur (e.g., due to application of many kV of electrical energy. The inputted energy can be thermal, mechanical (such as ultrasonic nebulization), or it can take other forms. In principle there is no reason why, if sufficient energy is inputted, so many droplets cannot be introduced into the vapor that nearly all water molecules will be involved or associated with them to some extent as a dynamic equilibrium between evaporating and condensing species is maintained. Thus in equations 16, 17, and 19, one could let $n_v + 1.0$ as an absolute limit as $s \rightarrow 1.0$, and could calculate corresponding maximum voltmeter readings, E_v , that could be measured under these limiting conditions. In the example for equation 20 at 25 °C, the voltmeter reading is calculated as $E_v = 10$ V dc. In recent UMIST experiments, almost precisely 10 V dc was measured as a maximum at 25 °C however much energy was supplied to the system. It could not be exceeded by inputting additional energy. However, if the energy input were relaxed, the reading fell below 10 V dc. At other temperatures, somewhat higher or lower voltmeter readings were obtained as $s \rightarrow 1.0$, but these readings agreed well with calculated values from the equations here for those temperatures and other conditions. Further, as the saturation ratio increased with humidification (e.g., by boiling or nebulizing liquid water), or as it decreased when vapor and droplet generation ceased, the readings closely followed the (s)¹³ dependency for E_v , and the corresponding $\sim(s)^{10}$ dependency (equation 21) for n_v . These results seem to indicate unequivocally that complete clustering of the vapor can be approached ($n_v \approx 1.0$) as $s \rightarrow 1.0$ using modest energy sources such as boiling water, ultrasonic nebulizers, or even in

very clean standing water systems like those that must be used to measure standard values such as saturation vapor pressure of water. Since the fraction of water vapor that is clustered, n_v , can now be calculated for given conditions, it is straightforward to derive the equation for the average molecular weight, M_{av} , of water vapor:

$$M_{av} = m \left[(1 - n_v) + n_v \cdot c_\mu \right] \quad (22)$$

where $m = 18$ = the molecular weight of a single monomer, $(1 - n_v)$ is the vapor fraction present as monomers and the fraction n_v is present in neutral clusters of mean "size" c_μ monomers. This rearranges to:

$$M_{av} = m \left[1 + n_v (c_\mu - 1) \right] \quad (23)$$

which can be written also as a function of the saturation ratio ($s, = \%RH/100$) from Equations 2, 3 and 21 as:

$$M_{av} \sim 18 \left[1 + (s)^{10} (c_\mu \cdot \sqrt{s} - 1) \right] \quad (24)$$

Note that if complete clustering is approached as saturation is approached in water vapor or moist air:

$$M_{av} = 18 (1 + c_\mu - 1) = 18 \cdot c_\mu \quad (S \rightarrow 1.0, n_v \rightarrow 1.0) \quad (25)$$

That is, the vapor molecular weight is simply 18 times the mean cluster size, a perfectly logical result that can also explain the very large value of water's latent heat of vaporization, ΔH_v . For example, at 25 °C $\Delta H_v = 10,500$ cal/g-mole based on an assumed molecular weight of $m = 18$. The mean size of the cluster distribution at 25 °C in saturation (where ΔH_v is measured) is $c_\mu = 12$ (equation 2). Thus from equation 25, the true value of ΔH_v 25 °C = $10,500/M_{av} = 10,500/(18)(12) = 48.6$ cal/g-mole, a latent heat value very much like that of other substances at 25 °C. Using equation 24, curves for values of M_{av} versus s at several temperatures can be calculated as in Figure 9.

Knowing n_v for given conditions, the effects of clustering on the partial pressure of water vapor also can be investigated. We know (as deBoer³ has reminded us) that water has a far lower vapor pressure than would be expected from classical theory for an ideal gas; one of the basic tenets of this theory is that the molecular weight of an ideal substance is unchanging.³⁵ Thus, the correct equations can be obtained from kinetic theory simply by correcting for the actual molecular weight of the vapor, M_{av} , for given conditions (equations 22-25). From the gas laws:

$$\frac{P}{V} = \frac{nRT}{MV} = \frac{WRT}{MV} \quad (26)$$

where n is the number of g-moles of a substance obtained by dividing its weight in grams, W , by its g-molecular weight, M . For pure water vapor of mass W in a given volume at a given temperature, we would like to be able to calculate

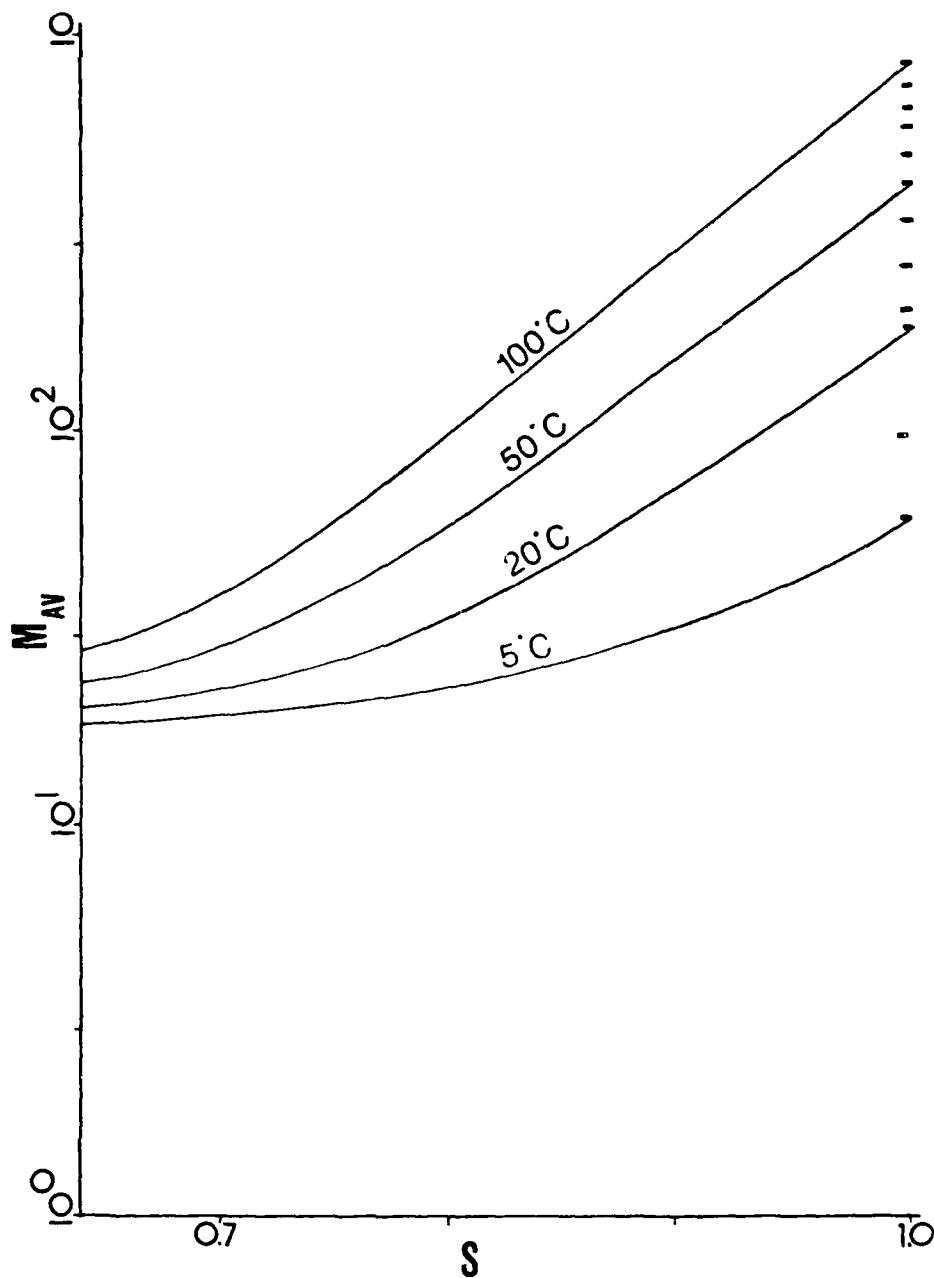


Figure 9. M_{AV} , The Average "Effective Molecular Weight" of Water Vapor vs. Saturation Ratio ($s = \% \text{ RH}/100$)

the vapor pressure that it would have if it were actually comprised of nothing but single water molecules (monomers), " P_1 ", thus,

$$\frac{"P_1"}{P} = \frac{WRT}{mV} \quad (27)$$

But, the weight of the vapor is divided into a cluster fraction w_c and a monomer fraction w_1 such that $W = w_1 + w_c$. The measured pressure is:

$$P = \frac{RT}{mV} \left[\frac{w_1}{(c=1)} + \frac{w_c}{c_\mu} \right] = \frac{RT}{mV} \left[\frac{(1 - n_v) + n_v}{(1)} \frac{1}{c_\mu} \right] = \frac{RT}{mV} \left[1 + n_v \left(\frac{1 - 1}{c_\mu} \right) \right] \quad (28)$$

Taking the ratio " P_1 "/ P from equations 27 and 28 gives:

$$\frac{"P_1"}{P} = \left[\frac{1}{1 + n_v \left(\frac{1}{c_\mu} - 1 \right)} \right] \quad (29)$$

or:

$$\frac{"P_1^\circ"}{P^\circ} = \frac{P^\circ}{1 + n_v \left(\frac{1}{c_\mu} - 1 \right)} \quad (s = 1) \quad (30)$$

for the saturated vapor ($s = 1$). For sub-saturated conditions:

$$\frac{"P_1"}{P} = \frac{(s)(P^\circ)}{1 + (s)^{10} \left(\frac{1}{c_\mu} - 1 \right)} \quad (31)$$

When we measure the saturation vapor pressure of water at any temperature, we are measuring P° . Our tables of saturation vapor pressure are tables of P° . Thus, we can calculate " P_1 " from equation 31 as is done for several temperatures in Figure 10. Note that as $s \rightarrow 1.0$ so that $n_v \rightarrow 1.0$ from equation 30:

$$\frac{"P_1^\circ"}{P^\circ} = c_\mu \quad (s \rightarrow 1.0, n_v \rightarrow 1.0) \quad (32)$$

Thus, kinetic theory tells us that if it were somehow possible to break the hydrogen bonds that hold the clusters of mean size c_μ together in saturated water vapor (equation 32), or for that matter in sub-saturated water vapor (Equation 31), a partial pressure substantially larger than standard equilibrium values would be measured. This would help to explain deBoer's³ rate of evaporation dilemma.

It would be very useful if other definitive experiments could be devised to measure " P_1 " and its steep humidity dependence, especially above $s = 0.9$ (90% RH) as seen in Figure 10. Asakawa³⁸ has reported that the application of an electric field of many kilovolts (kV) to a grid fixed some centimeters above a liquid water surface can greatly speed the rate of evaporation or raise the water vapor partial pressure substantially if this is done in a

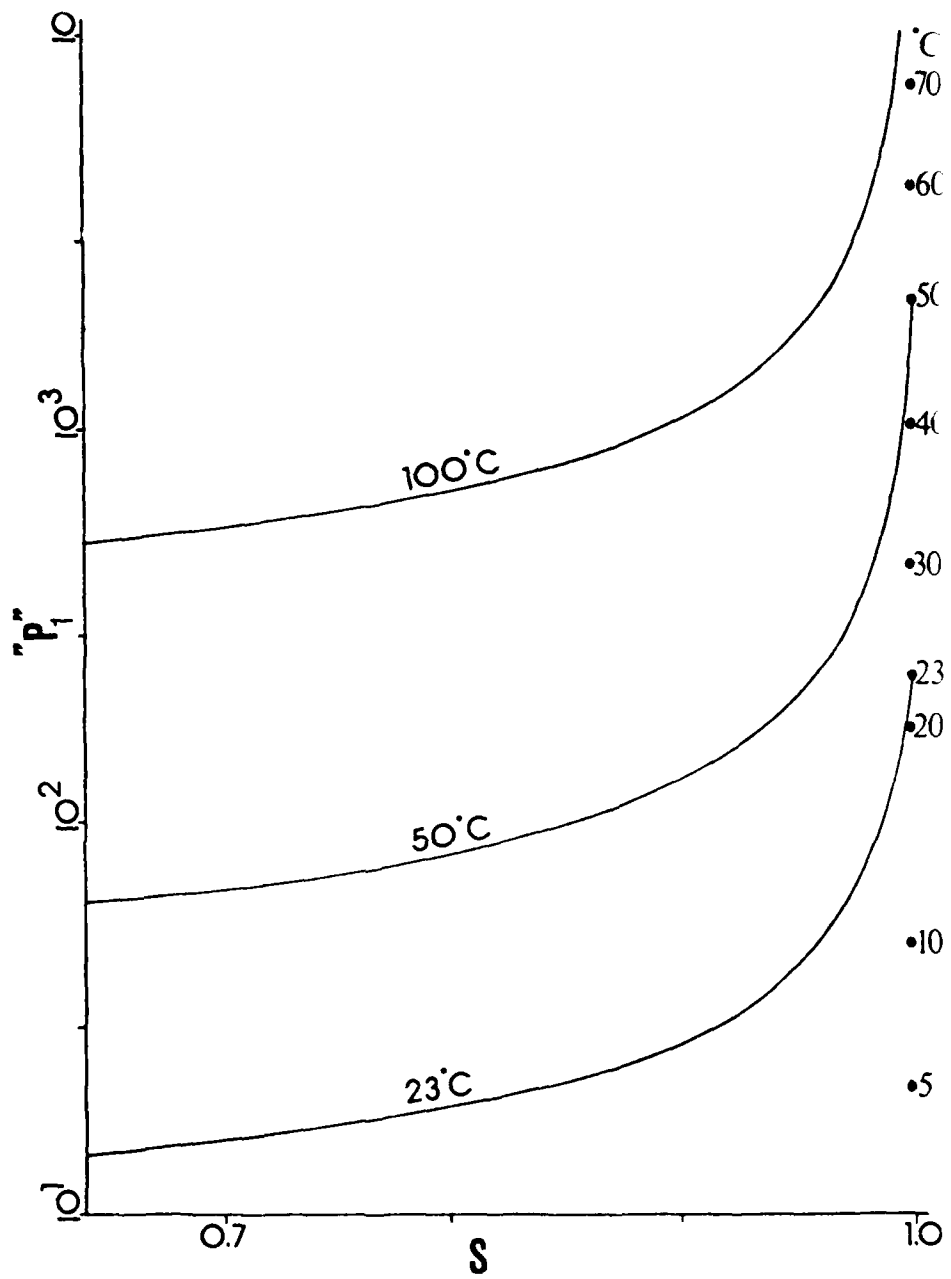


Figure 10. " P_1 ," In mm Hg (Torr), The vapor pressure that water vapor would have if it actually consisted of all monomers

closed container. Electrification of this kind is said to be used to speed drying in the Japanese commercial manufacture of rice cakes that are suspended in an electric field. Asakawa's results could be explained on the grounds that electrification breaks hydrogen bonds in vapor water clusters, thus raising the vapor pressure toward " P_1 " and in explaining also observed partial pressure increases in closed containers upon electrification of the vapor. Another explanation is that the electric field simply removes dissociative ions of water clusters in the vapor at a faster rate proportional to the applied kV, thus "pulling" the dissociative reaction of equation 1 to the right as the ions are swept away in the vapor, forcing neutral clusters to be dissociated at a faster rate in an attempt to maintain the equilibrium. It was mentioned earlier that the dissociative reaction of equation 1 could be "pushed" to the right by β -irradiating neutral clusters in water vapor, thus yielding much larger-than-equilibrium populations of water ion clusters like those whose mass spectra are seen in Figure 7. These mass spectra were obtained in exactly this way.

It is possible that both mechanisms can contribute to the observed partial pressure and electrical behavior of water vapor: (1) direct dissociation of hydrogen-bonded clusters at faster rates in sufficiently strong electric fields to approach " P_1 " (as suggested by Asakawa's data); (2) the sweeping away of water ions to force their dissociative replenishment by the neutral clusters, perhaps even in weaker electric fields.

If equation 10 is evaluated numerically, it is found that for typical equilibrium conditions in water vapor N_{CC} is enormous compared to I_{CC} . The neutral clusters (N_{CC}) outnumber their dissociative counterparts, the water ions (I_{CC}), by factors of 10^{10} to 10^{11} . Thus, enormous increases in the vapor ion population (moving to the right in equation 1) can be accommodated by using whatever energetic means are available. β -irradiation and field electrification are but two examples. In the denominator of equation 10, the concentration or population of the neutral species will indeed remain essentially unchanged (i.e., $a = 1$), thus this observation that justifies the definition of the dissociative ion product in liquid water even more applicable to the vapor than it is to the liquid. If the vapor ion populations can be shown to rise under energetic conditions and have already been shown to depend steeply upon humidity ($\sim f(s)^{13}$), the logical extrapolation of these data would be to the liquid phase. That is, the density difference would be eliminated at saturation at the vapor liquid interface, and the ion population in the vapor would simply approach that of the ion product of liquid water as determined by conductivity measurements of the liquid. These conductivity measurements are, incidentally, exactly analogous for the liquid and vapor phases. A 1 cm³ cell is standard for liquid measurements. For the present work, the large dimensions of our cell (Figure 1) are considered necessary to make up the density difference between the liquid and vapor phases.

Hoenig (written communication with S. A. Hoenig, University of Arizona, Tucson, AZ, 1981-86) briefly repeated Asakawa's vapor pressure measurements³⁸ and achieved immediate success. At 20 °C above standing water, taking no special precautions to purify it, he measured an increase of 13 mm Hg in the pressure "immediately" upon application of 22 kV above the liquid surface. Since the saturation vapor pressure at 20 °C is $P^{\circ} = 17.55$ mm Hg, this was a "significant" 74% increase. Interestingly, if Hoenig's relative humidity (which he did not measure) in his closed apparatus were about 92% ($s = 0.92$), his result would agree almost precisely with the " P_1 " value that can be estimated from Figure 10.

It is not unusual to obtain only 90-92% RH over standing water in contaminated systems. Thus, one wonders what extraordinary measures must be taken in precision measurements of the "standard" values of saturation vapor pressure that are widely tabulated. One infers (indeed, hopes) that the tabulated values do, actually, correspond to 100% RH ($s = 1.0$). In our own experiments as has been discussed, humidities above about 90% were not achieved without energetic means. And energetic systems are, of course, frequently non-equilibrium ones.

5. EXPERIMENTAL RESULTS (PART II)

The experimental results discussed earlier could not have been evaluated and explained without first developing a new theory of molecular clustering in water vapor. These new results were observed to give such close agreement with this new theory, as do results of measurements in several other scientific disciplines, that they essentially offered proof of the theory. Thus, we now have the tool to permit us to design new kinds of experiments to broaden our understanding of the physics of water vapor and to make the theory still more rigorous and quantitative.

One very useful investigation suggested by the theory would be that to determine to what extent the electrification of water vapor produces marked changes in the vapor structure. The work of Asakawa and Hoenig showed that high-kV electric fields could raise the vapor pressure of water vapor, suggesting either a breaking down of neutral clusters either directly or by a sweeping away of ions that had to be replenished by the dissociation of more neutral clusters at a faster-than-equilibrium rate. Both mechanisms would drive the dissociative reaction of equation 1 away from equilibrium, toward the right. The theory suggests three questions.

- What is the threshold voltage where an increase in ionization beyond the equilibrium value is just perceived, i.e., the beginning of "breakdown"?
- How does the ionization proceed at higher voltages above the threshold?
- How is the threshold voltage affected by the ambient temperature and humidity?

In our experimental apparatus, we can make these measurements very easily by varying the cell bias voltage (E_b), which has been fixed at $E_b = 400$ V dc for experiments reported thus far in this paper. The box (Figure 1) was dry at the start of each of these earlier experiments, i.e., it contained no standing liquid water.

A 0-2 kV regulated power supply (Brandenburg Model 475R) was added to the apparatus shown in Figure 1 and 2. This supply is switchable in steps of 100 V dc over its full output range. The 400 V dc power supply described earlier is continuously adjustable. Early in this work, it was verified that over this 0 - 400 V dc range, for typical ambient temperatures and humidities, the supply voltage produced singly-charged ions in proportional populations in the vapor. That is, plots of E_v versus E_b were perfectly linear as would be expected. It was thought that $E_b = 400$ dc was far below the voltage required to induce "electrical breakdown" as any deviation from such linear behavior in moist air

is popularly known. These trials were repeated recently with the same results. Using the 2 kV power supply, the bias was then increased in steps of 100 V dc to a maximum bias voltage of 2 kV. The results are shown in Figure 11, where additional details are given in the caption. Here, a "knee" is clearly seen in the measured ion population above (only) 1 kV. Other experimental curves for lower humidities and somewhat different temperatures also are shown. Temperature has much less effect than humidity in determining the location of these curves. The knee or intercept with the linear E_y versus E_b bias line is seen for these curves to suggest that this intercept moves somewhat to the left, i.e., to lower bias voltages E_b with increasing humidity.

Figure 12 shows many new data points taken at bias voltages of $E_b = 0.5, 1.0, 1.5$, and 2.0 kV on the familiar coordinates of Figures 3, 5, and 6. Note that the abscissa is expanded here to show better detail of the experimental data over the humidity ranges used; thus, the $f(s)^{13}$ slope here appears more shallow than in the earlier figures on the same coordinates. Figure 12 reveals the entire, previously unrecognized, picture to us. The lower curve for $E_b = 0.5$ kV will be exactly the same for bias voltages ranging from very low ones up to those where the knee is observed (Figure 11). Data points are observed in Figure 12 along horizontal lines extending to the left to lower humidities. The box was wet in these experiments (standing water was present). Thus, these data show that a zero-slope condition for low humidities is achieved when liquid water is present to replenish equilibrium water vapor concentrations by evaporation. This indicates that data points below about $E_y = 0.03$ V dc for previous dry box conditions corresponded, in fact, to non-equilibrium conditions, where except by moist air leakage from ambient air outside the box no source of neutral cluster replenishment to equilibrium levels was available. The lower points in Figure 5 do appear to be equilibrium ones, however. A horizontal "tail" at lower humidities is predicted by theory for equilibrium conditions corresponding to the linear regions of the E_y versus E_b curve (Figure 11), as is easily verified by a few example calculations. In particular, heating experiments tend to drive ion populations below equilibrium values once the water (liquid) introduced during evaporation has evaporated completely. As the bias voltage is increased to $E_b = 1.5$ kV and especially to 2.0 kV in Figure 12, it is observed that departing data points from the curves becomes more pronounced. The vertical bars on the top curve do not represent experimental error; rather, they show measured "jumps" in the experimental readings for the conditions shown. These jumps repeat several times as given conditions are maintained briefly during changes in temperature and especially humidity in the box. They are thought to correspond to avalanche-like changes in cluster size distributions and populations as previously-stable ones are stressed, especially for those mean cluster sizes that represent favored low-energy cluster geometries. The top curve in Figure 12 also shows a pronounced flattening toward higher humidities, perhaps indicating that some sort of limiting conditions was being approached at this highest bias setting in these experiments.

The data points in Figure 12 were very carefully taken. Thus, their spread is evidence of the wide range of "hysteresis" effects in water vapor about equilibrium measured in these experiments. This probably arises from the fact that equilibria of neutral clusters have to be maintained by far smaller ($10^{-11} - 10^{-10}$) populations of the water ions which will be addressed in the

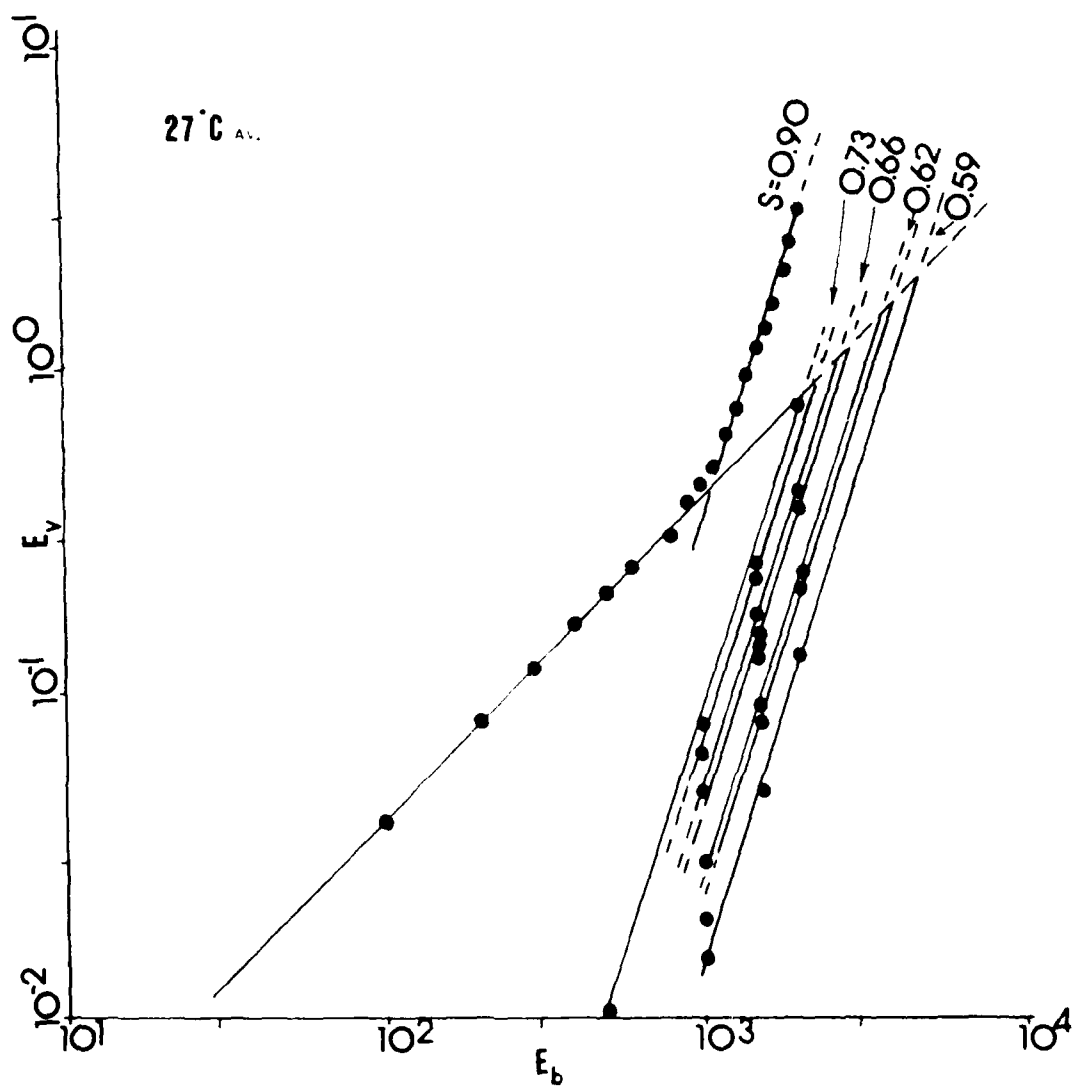


Figure 11. Data Plots of Voltmeter Reading, E_v , vs. Supply Voltage, E_b , for Increasing Bias Voltages $E_b = 0.1 - 2.0$ kV Under Conditions of an Initially Wet Box

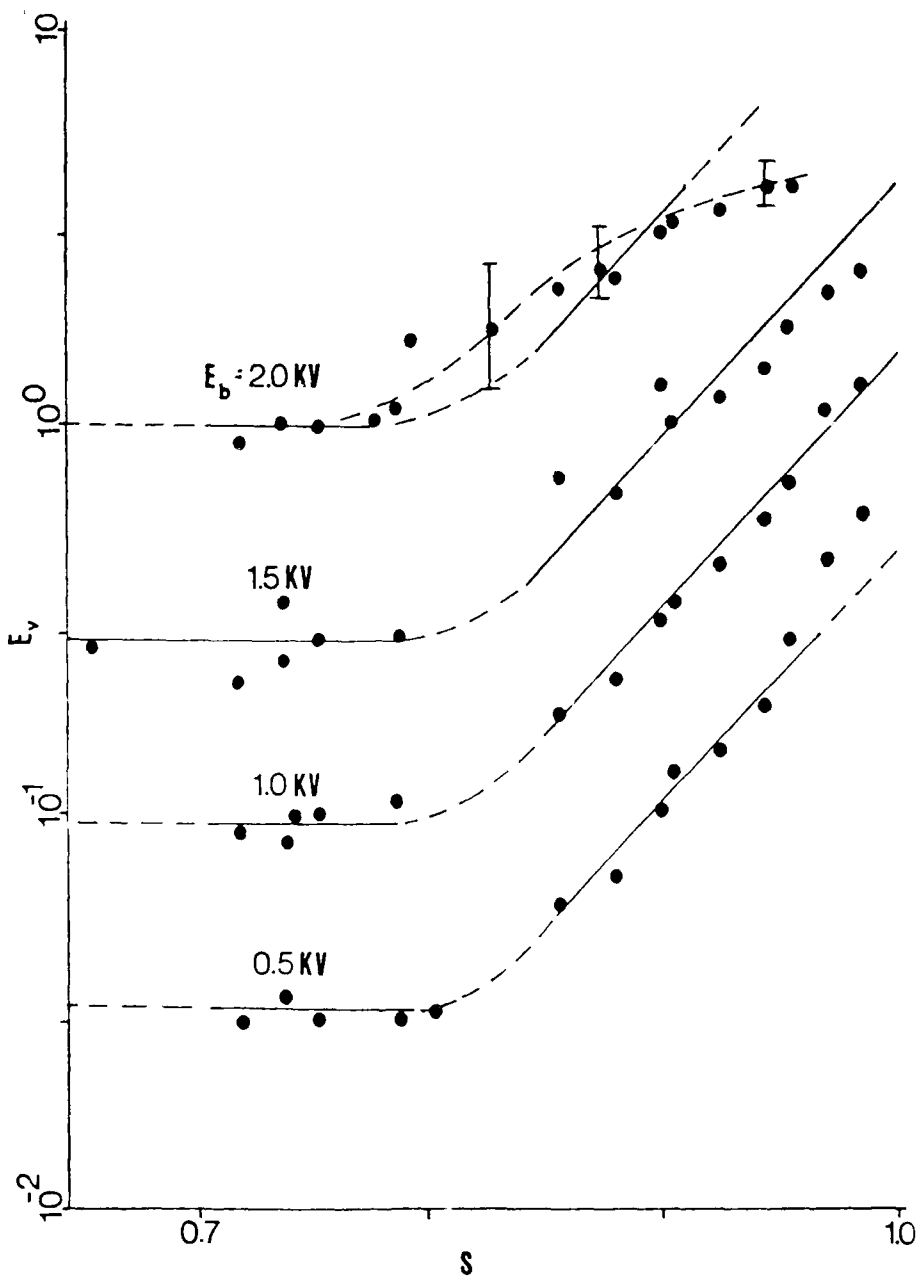


Figure 12. Data Plots of Voltmeter Reading, E_v , vs. Saturation Ratio Obtained By First Heating Moist Air in an Initially Wet Box to a Maximum Temperature of 33 °C

closing discussion. It would be difficult to identify any other equilibrium system for which the populations of the species on either side of the reaction equation (equation 1) are so mismatched. Enormous, previously-uncharacterized populations of neutral water clusters and their dissociative ions have been shown to exist at all times in water vapor and moist air. It is perhaps understandable that their populations about equilibrium values are so unstable especially under changing conditions so as to have added considerably to the task of establishing their very existence, much less their behavior.

It is worthwhile to conclude this discussion with a description of exactly the mechanisms that account for water cluster and ion equilibria in water vapor and moist air. These mechanisms operate over a wide range of conditions from those of fog and cloud, where equilibria are most easily approached, to those of high temperatures and low humidities, where equilibria can be lost for long periods of time.

Under prolonged stable conditions, a given neutral cluster can have an indefinite lifetime, although the monomers comprising it will be constantly changing in the sub-millisecond timeframe of dissociative ion lifetimes and the making and breaking of intermolecular hydrogen bonds. Changing conditions severely stress cluster equilibria. During heating, e.g., the cluster populations and their size distributions respond immediately, the neutral cluster population N_{CC} can fall precipitously over many orders of magnitude. Once dried, the vapor sample can be restored to a higher humidity by cooling or by mixing with moist air. This requires the restoration of huge populations of neutral clusters previously lost in the drying process. There are always enough dissociative ions in the vapor to accomplish this, and other "foreign" nuclei may also be present to speed the process. Thus, the rate of evaporation becomes critically important if the rebuilding of the neutral cluster population (N_{CC}) is to keep pace with the rate of humidification; i.e., if dynamic equilibrium is to be maintained. Recent experiments at UMIST show this unequivocally. If humidification by ultrasonically-nebulized cold water mist is not energetic enough, the rate of cluster production can fall behind the rate of humidification (Figure 4) by many minutes. This corresponds to conditions such that larger-than-equilibrium populations of monomers are in the vapor, awaiting ionic nuclei about which they can swarm and cluster. This condition usually corrects itself within several minutes. For example, if the source of humidification is simply standing water in contact with the unstirred vapor, the rate of humidification initially is high but slows after 5-10 min from the moment liquid water is introduced into the system. The relative humidity then becomes asymptotic to about $s = 0.9$ (90% RH) at room temperature.

At the same time, the cluster population climbs steeply to regain equilibrium conditions at this maximum attainable humidity. There, the rate of evaporation over standing water maintains the corresponding equilibrium cluster population for these conditions. But, maximum cluster populations at a given temperature for saturated vapor cannot be achieved without energetic humidification, e.g., by nebulizing or by boiling water under atmospheric conditions, except above about 50 °C where spontaneous nucleation¹⁹ insures that droplets are always present in the vapor to assist in the attainment of equilibrium.

When liquid water and its vapor are together in a small closed container at atmospheric pressure, the extent of mixing between the liquid and vapor phases can be enhanced by energy supplied to the system. At rest, an equilibrium will be slowly approached between evaporating liquid and recondensing vapor, measured as the saturation vapor pressure, a fundamental physical property of water at any temperature, that increases as the temperature (energy) of the system increases. As more energy is supplied to the system, liquid water can be made to appear in the vapor in direct proportion to the amount of energy expended. For example, the liquid can be heated to boiling with attendant eruption of vapor bubbles from within the body of the liquid and production of steam and aerosol in proportion to the rate of heat (thermal energy). Liquid water can be sprayed through high-pressure nozzles to produce large populations of droplets in the vapor phase (mechanical energy). An ultrasonic transducer can be used to nebulize large populations of liquid droplets into the vapor (acoustic energy - arguably, another form of mechanical energy).

Under such conditions, liquid water species in the vapor will include large, clearly visible droplets, finer droplets near or below optically-detectable size, and condensing or evaporating species down to those of sub-critical size for droplet nucleation, i.e., hydrogen-bonded molecular clusters ranging from sizes of about 45 water molecules (monomers) down to much smaller sizes and to individual monomers. Consider the fate of a single liquid droplet originally introduced by some energetic means into the vapor. It will evaporate from clearly visible diameter, where it can carry many electrical charges, through the size range where surface tension and electronic charge offset one another and a Rayleigh "explosion" occurs creating several new sub-droplets that can also carry multiple charges. Each sub-droplet will evaporate further until sub-critical size is reached below about 45 monomers, where it is generally conceded that only a single electronic charge can be carried by each "droplet" or molecular cluster if it is an ion. It can, of course, also be an electrically neutral, uncharged cluster of sub-critical size commonly referred to as a neutral water cluster.

Such clusters, be they neutral or singly-charged at any instant, are cross-linked by short-lived hydrogen bonds that couple the monomers together. The binding energy of each hydrogen bond is on the order of 0.1 - 0.2 eV. Since the clusters adopt the most compact configuration for any size, the number of hydrogen bonds instantaneously linking monomers in larger clusters will be greater than the number of monomers held together. For example, from simple geometric considerations, there can be as many as 90 hydrogen bonds in a cluster of size 32 monomers, 30 bonds in one of size 20, 12 in one of size 6, 8 in one of size 5, and 6 in one of size 4. Only when a cluster becomes smaller than 4-6 monomers, a single electronic charge (about 1 eV) would be as effective as the hydrogen bonds in holding the cluster together at any instant of time. Other measurements of water clusters have shown that a cluster of only 4-6 monomers already exhibits the thermodynamic properties of bulk liquid water due to hydrogen bonding,¹⁸ even though the critical size for liquid droplet nucleation is about 10 times greater. Thus, larger clusters are held together momentarily by their hydrogen bonds even when uncharged with a binding energy equivalent to that if they carried many electronic charges. In very large, sub-critical clusters, therefore, the presence of a single electronic charge, whether a cluster is an ion cluster or a neutral one, makes very little difference to its instantaneous stability and, hence, to its lifetime. But, once dissociation of

a neutral cluster begins (equation 1), ions are produced that are instantly swarmed by water monomers, thus tending to re-build the cluster and stabilize the equilibrium.

If extensive clustering can be caused in water vapor by the energetic evaporation of liquid water, we are drawn back again to question what conditions actually exist in stagnant, closed systems of liquid water and its vapor, such as those used to measure the saturation vapor pressure of water that is a fundamental physical property and can be measured with great precision as a function of temperature. We know that above about 50 °C, spontaneous nucleation of droplets occurs in water vapor even of the highest purity at saturation; so, it is clear that at these higher temperatures with optically-detectable droplets always present in the saturated vapor, a significant fraction of the vapor n_v must be clustered. As the atmospheric boiling point is approached, free exchange of droplet formation and evaporation occurs. It would not be unreasonable to surmise that $n_v + 1.0$ has, indeed, been indicated in saturated moist air even at much lower temperatures in the experimental measurements reported here. A study of precision techniques used to measure "standards" of saturation vapor pressures of water might be in order, in this respect.

Finally, we observe that when the temperature falls to 0 °C, Figure 2 and equation 2 indicate that the mean size of the cluster distribution reaches unity (the monomer). Similar conditions are predicted at somewhat higher temperatures and lower humidities by equation 3, e.g., $c_\mu = 1$ for $s = 0.28$ (28% RH) at 2 °C and for $s = 0.13$ at 4 °C. But, it is important to realize that although the mean size, c_μ , is an invaluable tool in our analyses here of Gaussian-like cluster size distributions, the extrapolation of the mean to unity at 0 °C, $s = 1$, does not mean that huge cluster populations do not continue to exist in water vapor or moist air. Consider the cluster distributions shown in Figure 7, where a vertical line can be drawn through the mean size, and the left-hand side of a distribution can be simply cut off along this line and discarded. The remaining, right-hand side of the distributions are Boltzmann-like, i.e., they have shapes like those normally associated with distributions of much smaller, collision-induced dimers, trimers, etc. Now consider what these halved, right-handed distributions would look like for conditions that really do exist near 0 °C. The dimer would be the most populous species both in the collisional and evaporative size spectra. But the mass spectra of the larger cluster sizes would merge with those of collisional dimers, trimers, etc., and so would fall in population much more slowly than predicted by collisional theory only.⁴ Such mass spectra are regularly observed,¹⁸ but often are attributed to collisional mechanisms. Thus, even at minus 20 °C (-20 °C), where equation 2 predicts that saturated vapor would have a mean cluster size of "minus 7.8" ($c_\mu = -7.8$), Boltzmann-like distributions of neutral clusters above size 8 would still exist and could carry on their normal equilibrium activity, although reduced but still huge populations.

From all of this, it would seem reasonable to surmise that the cluster fraction in water vapor or moist air, n_v , for conditions where the vapor is in contact with its liquid, can approach unity as saturation ($s = 1$) is approached, and that this fraction has a further $\sim (s)^{10}$ dependency at any temperature when saturation is not attained (equation 21).

6. CONCLUSIONS

The unequivocal experimental results and their agreement with the new theory developed from first principles in this paper, can be explained only by the existence of enormous populations of neutral water clusters in the vapor, which are in equilibrium under average conditions with their dissociative ions (equation 1). This finding agrees with those of a great many other scientific disciplines and, in fact, gives the only consistent explanation of all such observations that have been reported from such diverse fields as cloud microphysics, mass spectrometry, IR and millimeter-wave absorption spectroscopy, cluster modeling, atmospheric electricity including insulator effects, electrical conductivity, and thermodynamic measurements of water clusters and water itself. Many references to the best of these measurements have been given and addressed briefly here. There is simply not enough space to list and to discuss all of them. C. T. R. Wilson knew in 1897 of the existence of these huge neutral cluster populations,⁵ but could not explain them because hydrogen bonding was then unknown so he proposed that the water molecule radius might be three times larger than it actually is. The ratios of Wilson's populations of water ions to neutral clusters, within limits of his apparatus, were nearly identical to those measured and reported here. The existence of spontaneous nucleation¹⁹ in warm moist air, however clean, at atmospheric pressure is impossible to explain except by the presence of large clusters in large numbers in water vapor. Homogeneous nucleation theory⁴ cannot explain this.

Intensive research is continuing at UMIST on this important problem. In recent work, ion measurements have been carried to supply voltages of up to 20 kV or more, and into the realm of corona discharges in moist atmospheric air. Many new observations have been made that confirm independently the correctness of the water cluster theory presented here. For example, measurements of increased water vapor partial pressure (like " P_1 ") have been made at incipient corona voltages, thus confirming the observations of Asakawa³⁸ and Hoenig (conversation with S. A. Hoenig, 1981-1986). Supply currents as well as cell and supply voltages have been measured, and the electrical energy generated per cubic centimeter of vapor can be calculated. It is found that, just at the onset of corona, electronvolts of energy are available for each neutral cluster in the enormous population, N_{cc} ; thus sufficient energy is available to dissociate many hydrogen bonds per cluster or to ionize clusters (equation 1). This suggests that corona itself (and lightning) in moist air is the manifestation of the breakdown of neutral cluster populations under the applied potential gradient. Calculations have been made of the heating and cluster dissociation effects of electrical energy per cubic centimeter of vapor at incipient corona, and the manner in which these are offset by cooling due to "evaporation" of dissociated neutral clusters, so that the overall effect on the partial pressure increase measured can be assessed. It has been found that the two effects are nearly equal in magnitude, so that the resulting pressure that is read is much less than " P_1 " but rather represents a "balance" between the opposing pressure forces. Thus, the pressure differential read is a very sensitive indicator of the neutral cluster fraction, n_y , remaining in the corona as a function of applied voltage gradient. As would be expected, n_y decreases as the voltage (and pressure differential) increases; typical values in the corona are $n_y = 0.1-0.2$, compared to 0.4 or more just below the corona voltage, or to values approaching unity in normal atmospheric air approaching saturation in the presence of liquid droplets. It is also found

that the heat of vaporization of liquid water can be used directly in the cluster calculations because clusters larger than 4-6 are thermodynamically liquid-like.^{17,18} Therefore, all evidence continues to suggest that clusters in water vapor and in the liquid are very similar except for their phase density (i.e., population per cubic centimeter differences). The dissociation reaction of equation 1 represents more a dissociation of individual clusters at any instant of time than of the phase in which they happen to be found.

Blank

LITERATURE CITED

1. Frank, H.S., In Water: A Comprehensive Treatise, Vol. 1, F. Franks, ed., Plenum Press, New York, NY, pp 515-543, 1972.
2. Luck, W.A.P., In Water: A Comprehensive Treatise, Vol. 1, F. Franks, ed., Plenum Press, New York, NY, pp 209 ff, 1972.
3. deBoer, J.H., The Dynamical Character of Adsorption, Oxford Press, Clarendon, England, 1953, p 16.
4. Abraham, F.F., Homogeneous Nucleation Theory, Academic Press, New York, NY, 1974.
5. C.T.R. Wilson, Philos. Trans. Vol. 189, p 265 (1897).
6. C.T.R. Wilson, Philos. Trans. Vol. 192, p 403 (1899).
7. Wilson, J.G., Principles of Cloud Chamber Technique, pp 1-29, Cambridge University Press, England, 1951.
8. Croxton, C.A., Statistical Mechanics of the Liquid Surface, pp xi and 198-218, Wiley Interscience, New York, NY, 1980.
9. Bignell, K.J., Quart. J. Roy. Meteorol. Soc. Vol. 96, pp 390-402 (1970).
10. Varanasi, P., Chou, S., and Penner, S.S., J. Quant. Spectrosc. Radiat. Trans. Vol. 8, pp 1537-1541 (1968).
11. Gimmestad, G.G., and Gebbie, H.A., J. Atmos. Terr. Phys. Vol. 38, p 325 (1976).
12. Wolynes, P.G. and Roberts, R.E., Appl. Opt. Vol. 17, p 1484 (1978).
13. Carlon, H.R., Infrared Phys. Vol. 19, pp 49-64 (1979).
14. Carlon, H.R., J. Atmos. Sci. Vol. 36, pp 832-837 (1979).
15. Emery, R.J., Zavody, A.M. and Gebbie, H.A., J. Atmos. Terr. Phys. Vol. 42, p 801 (1980).
16. Gebbie, H.A., Nature Vol. 296, pp 422-424 (1982).
17. Vernon, M.F., Krajnovich, D.J., Kwok, H.S., Lisy, J.M., Shen, Y.R., and Lee, Y.T., J. Chem. Phys. Vol. 77(1), p 47 (1982).
18. Mark, T.D. and Castleman, A.W. Jr., "Experimental Studies on Cluster Ions," In Advances in Atomic and Molecular Physics, Vol 20, Academic Press, New York, NY, pp 65-172, 1985.
19. Carlon, H.R., J. Phys. D: Appl. Phys. Vol. 17, pp 1221-1228 (1984).

20. Volta, A., Phil. Trans. Roy. Soc. Vol. 72, pp 237-280.
21. Faraday, M., In Electrostatics and Its Applications, p 402, A.D., Moore, ed., Wiley Interscience, New York, NY, 1973.
22. Lenard, P., Ann. Phys. Vol. 46, pp 584-636 (1892).
23. Simpson, G.C., Phil. Trans. A. Vol. 209, pp 379-413 (1909).
24. Nolan, J.J., and Enright, J., Proc. R. Dublin Soc. Vol. 17, pp 1-11 (1922).
25. Blanchard, D.C., The Electrification of the Atmosphere by Particles From Bubbles in the Sea, Woods Hole Oceanographic Institute, Reference 61-9, 1961.
26. Carlon, H.R., J. Appl. Phys. Vol. 51(1), pp 171-173 (1980).
27. Carlon, H.R., J. Chem. Phys. Vol. 78(11), pp 5523-5529 (1982).
28. Carlon, H.R., J. Chem. Phys. Vol. 78(3), pp 1622-1624 (1983).
29. Moore, A.D., ed., Electrostatics and Its Applications, pp 390-398, Wiley Interscience, New York, NY, 1973.
30. Roberts, R.E. Selby, J.E.A. and Biberman, L.M., Appl. Opt. Vol. 15, pp 2085-2090 (1976).
31. Carlon, H.R., Infrared Physics Vol. 22, pp 43-49 (1982).
32. Chalmers, J.A., Atmospheric Electricity, pp 85-88, Pergamon Press, London, 1967.
33. Israel, H., Atmospheric Electricity, Vol. 1, Israel Program for Scientific Translations, Jerusalem, 1971.
34. Carlon, H.R., and Harden, C.S., Appl. Opt. Vol. 19, pp 1776-1786 (1980).
35. Maron, S.H., and Prutton, C.F., Principles of Physical Chemistry 4th ed., pp 449-451, Macmillan, New York, 1965.
36. Holzapfel, W., J. Chem. Phys. Vol. 50, pp 4424 (1969)
37. Carlon, H.R., J. Atmos. and Terr. Phys. Vol. 44, pp 19-23 (1982).
38. Asakawa, Y., "Behavior of Fluids Under Electric Field," In Charge Storage, Charge Transport and Electrostatics with their Applications, Elsevier Publishing, New York, NY, pp 89-92, 1972.